

**UNITED STATES DEPARTMENT OF THE INTERIOR
GEOLOGICAL SURVEY**

**BEAUFORT SEA COASTAL EROSION,
SHORELINE EVOLUTION,
AND SEDIMENT FLUX**

By

Erk Reimnitz, Scot M. Graves, and Peter W. Barnes

Open-File Report 85-380

**This map is preliminary and has not been reviewed for conformity with
U.S. Geological Survey editorial standards and stratigraphic nomenclature.**

1985

ABSTRACT

A comparison of two editions of 1:50,000-scale NOS charts covering 344 km of coastline provides the basis for a detailed study of coastal erosion occurring over a 30-year period. This study also determines patterns in coastline evolution and their probable causes, and sediment yields from erosion. Excluding the large Colville Delta, advancing on average +0.4 m/yr, the average erosion rate is -2.5 m/yr. Extremes for the long-term average rates range up to -18 m/yr. The coastal plain deposits in one third of the study area are fine-grained mud, with an average erosion rate of -5.4 m/yr. The remaining region is composed of coarser sandy deposits, which erode on average -1.4 m/yr. Thus grain size of bluff material exerts the dominant control on coastal retreat rates. Other important factors include bluff height, ice content and thaw settling, bluff orientation, and degree of exposure to the marine environment. Vertical crustal motion has not played an important role during Holocene time. In calculating sediment yield we treat not only the materials above sea level, but consider that the marine profile to 2m depths is in dynamic equilibrium, and therefore contributes to the sediment yield. The upper part of the eroded section contains up to 75% ice, and the sediment yield is reduced accordingly. The annual yield from coastal retreat thus calculated is $2.5 \times 10^6 \text{ m}^3$, with the offshore contribution slightly higher than the onshore contribution. We estimate the annual sediment yield from the adjacent drainage areas is slightly less at $2 \times 10^6 \text{ m}^3$.

Studying the recent trends in coastal retreat, and the controlling factors, allows estimating the configuration and location of past and future coastlines. The evolution of coastal embayments and lagoons does not begin with the breaching and coalescence of large lakes, followed by thaw settlement. Rather, the existence of old, coarse-grained, and erosion-resistant barrier island and beach deposits exerts a strong influence on the locus and shape of some of the newly forming embayments, while others remain unexplained.

If the present coastal retreat rates have been sustained since sea level rise stabilized about 5,000 yr BP, then the corresponding ancient shoreline could have ranged from 7 to 27 km seaward of the present one at that time, in accordance mainly with grainsize variations in coastal bluffs. Furthermore, if erosion were operative only to 2-m water depths, as assumed in our sediment yield calculations, 10-20 km wide shallow platforms should be widespread around the Arctic Ocean. Since such platforms do not exist, and since we can show that thaw settling contributes very little to the shape of the marine profile, coastal retreat must be associated with erosion reaching to depths much greater than 2 m. The sediment yield therefore should be manyfold larger than we calculated. A growing body of evidence shows that the inner shelf seaward to at least 20-m depth is indeed an eroding surface truncating older strata. Considering the rapid, and deep-reaching erosion, modern deposits found in some of the shallow bays and lagoons cannot serve as sediment sinks to accommodate the materials introduced at the present (Figure 2). The sediment yield from coastal retreat and rivers largely by-passes the shelf. A 2-3 m thick sediment layer draping large regions is a result of ice-keels plowing into underlying strata, mixing these with modern materials and fauna into a transient "roto-till" unit.

Within the conterminous United States, the Gulf of Mexico coast has the highest erosion rates. The Texas coast, in many respects similar to that of the Beaufort Sea, retreats on average ~ 1.2 m/yr, or about half the Beaufort Sea average. Since coastal erosion in arctic regions is restricted to three summer months when waves and coastal currents are active, erosion rates there must be multiplied by a factor of four for a meaningful comparison with the Texas coast, which experiences waves and currents year round. Accordingly arctic erosion rates are 8 times higher than Texas rates. Additionally, arctic fetches commonly are restricted by the ever present polar pack, unlike the long and constant Texas fetch allowing generation of larger and more pervasive waves. Classic wave theory therefore can not wholly account for the sediment dynamics of the arctic coastal zone, and we are left with fundamental questions which are important to future coastal development by petroleum industry.

TABLE OF CONTENTS

INTRODUCTION	1
REGIONAL SETTING.....	1
Physiography and surficial deposits	1
Wave exposure	2
Shore processes.....	2
METHODS	4
Generalized nearshore geometry	5
Sediment yield from bluff erosion	5
Sediment yield from offshore erosion	5
Special case geometries.....	6
RESULTS	6
DISCUSSION.....	7
Regional patterns in erosion rates.....	7
Formation of embayments and lagoons by thermal collapse	9
Thermal collapse resulting in coastal sediment sinks	10
An example from the East Siberian Sea.....	10
Analysis of a North Slope profile	11
Vertical shelf erosion by shifting of the "equilibrium profile"	13
Total sediment yield from rivers and from coastal erosion	14
Inner shelf erosion a major sediment contributor	14
Comparison with erosion rates in the Gulf of Mexico.....	16
AKNOWLEDGEMENTS	17
APPENDIX	33
REFERENCES CITED	53

BEAUFORT SEA COASTAL EROSION, SHORELINE EVOLUTION, AND SEDIMENT FLUX

By

Erk Reimnitz, Scot M. Graves, and Peter W. Barnes

INTRODUCTION

Two sets of charts published by the U.S. Hydrographic Service and the National Ocean Survey, showing the shorelines for 1950 and for 1980 respectively, are compared in this study of Alaska's north coast between Drew Point and Prudhoe Bay. The mapping was done in accordance with national standards at a scale of 1:50,000, large enough to allow accurate and comprehensive delineation of coastline changes within the 30 year period (see accompanying mapsheet).

Previous studies (Dygas and Burrell, 1976; Lewellen, 1977; Hopkins and Hartz, 1978; Cannon, 1979; Kovacs 1983; and Naidu 1984), using largely spot measurements from aerial photos and maps (for example fig. 4), have documented rapid rates of coastal retreat (figures 2 through 21 are found on the mapsheet numbered sequentially in an easterly direction along the coast). They also have pointed out large regional differences and rapid changes in island configuration and location over various time spans.

The new 30 year comparison entails complete coverage of the coast within the study area (fig. 1) and allows an accurate determination of coastal erosion rate patterns. The coastal erosion rates together with the yield from upland sources are used to estimate the minimum amount of sediment supplied from the study area to the Beaufort Sea. An attempt was also made to interpret trends in coastal evolution in light of what is known about the unique high latitude modern shelf environments. Attempts to extrapolate paleo shorelines from the presently high transgression rates forced consideration of the continental shelf profile, and its evolution through time. These considerations lead to the realization that the arctic marine environment contains elements that are more erosive than its low-latitude counterpart, partly through the abrasive action of sea ice.

REGIONAL SETTING

Physiography and Surficial Deposits

The coastal plain in the study area is a vast, flat, tundra-covered surface with thousands of shallow (1-2 m) thaw lakes (figs. 3, 20). Along the coast this surface is only 2 to 6 m above sealevel, and rises imperceptibly to the south (figs. 5, 17). The tundra surface is underlain by the Quarternary Gubik Formation (Black, 1964) whose marine, alluvial, and glacio-fluvial sediments are mantled by 2-3 m of late Pleistocene and Holocene thaw-lake deposits, consisting mostly of peat and mud (Williams, et al., 1977). Except for an up to 30 cm thick surface layer, the materials underlying the tundra surface are permanently ice bonded. They contain 60 to 70% of ice in the interstices, and in the form of small but pervasive sub-horizontal ice lenses in the upper several meters. In addition, these upper sediments contain 10 to 20% ice in the form of massive ice wedges (fig. 9 and 10) (Sellmann, et al., 1975). Sandy gravel beaches fronting the coastal bluffs generally are about 10 m wide (figs. 6, 11, and 18) and only several tens of cm thick. The active mouths of the Kuparuk and the

Colville Rivers are marked by very low mud flats (figs. 13 and 20), whereas the inactive distributaries are generally marked by 1 m high tundra covered surfaces (fig. 12). About 5 to 8 km from shore an island chain stretches from Harrison Bay to Prudhoe Bay. These are mostly low (1-2 m high) and narrow barriers composed of sand and gravel. Pingok, Bodfish, Bertoncini, and Cottle Islands are exceptions in that they contain remnants of the tundra-covered coastal plain with higher elevations corresponding to adjacent land areas (figs. 18 and 20). Harrison Bay and the stretch of coast from Cape Halkett to Drew Point are not protected by islands, with the exception of the sand bar across the large breached lake at Pogik Bay (fig. 3).

The 2-m isobath, which roughly corresponds to the ultimate thickness of the seasonal fast ice, marks a distinct change from a flat inshore bench to a steeper-sloping seaward profile. The outer edge of this so called "2m bench" (Barnes and Reimnitz, 1973) is often slightly shallower than the waters some distance landward. We include this feature on the comparative maps (sheet 1) and in our sediment budget calculations as its outer edge is 1) an important morphologic feature (Reimnitz and Bruder, 1972), 2) the boundary between texturally well sorted sands inshore, and poorly sorted sandy muds offshore (Barnes and Reimnitz, 1973), 3) controls sea ice zonation (Reimnitz, et al., 1978), and 4) is the outer boundary to which seasonal bottom freezing occurs (Reimnitz and Barnes, 1974). In Harrison Bay the 2m bench is up to 10 km wide, elsewhere it is only 0.5 to 5 km wide.

Wave Exposure

The sea surface is completely ice covered for 9 months each year (fig. 3) and even during the short open-water season fetch and waves are minimized by the abundance of drifting ice (figs. 14B and 20). On any usual summer day a skiff can therefore safely land on a seaward-facing beach (fig. 19), while in the lagoons the relatively ice-free conditions lead to greater wave activity. Winds from the northeast dominate, and movement of the littoral drift, coastal currents, and ice drift are to the west (U.S. Department of Commerce, 1981, p.57). Even during rare periods when much of the continental shelf is ice free some grounded ice will usually collect and remain in the nearshore zone.

Shore Processes

Nummedahl (1979) reviewed available littoral transport estimates and concluded that the average transport is westward at a rate of "a few tens of thousands of cubic meters per year". A more thorough evaluation of Beaufort Sea coastal processes by Owens, et al., (1980) quotes a transport rate of 2,000 to 5,000 m³/yr. Reimnitz and Kempema (1983) give similar transport rates for bedload material in a several kilometer wide coastal belt, based on measurements made along the outer part of the 2m bench, several kilometers from shore. This transport again is mainly to the west due to prevailing easterly winds.

The sediment transport is not driven by waves and currents alone. Grounded ice in the nearshore seems to play a more important role in various ways besides its bulldozing action. When worked by storm waves (fig. 16A), this ice acts to intensify turbulence resulting in increased sediment suspension and transport, and a highly irregular "ice-wallow relief" is imparted to the beach and shoreface (Reimnitz and Kempema, 1983) (figs. 7 and 16). This irregular relief in turn when attacked by normal waves results in increased bottom instability, sediment re-suspension, and transport. During open-water storm conditions these combined processes can act in a coastal belt up to 1000 m or more wide, bringing about accelerated bottom erosion and thereby steepening of the foreshore. This in turn can result in accelerated coastal retreat. Under such conditions as much as 30m of coastal plain deposits can be eroded within a period of several days (Short, et al., 1974).

With the coastal deposits being ice-bonded and air and ocean temperatures near the freezing point, factors other than the energy level of the marine environment affect coastal processes. In

this environment unique processes occur. In most cases retreat of the coastal bluffs involves the process of thermo-erosion which includes the following: a) formation of a thermo-erosional niche, when a turbulent sea is brought in contact with bluffs (figs. 9, 10, 11, and 18), b) collapse of bluff materials (figs. 2 and 5), c) slumping, and d) saturated flow of thawed sediments. The mechanisms are described in detail by Harper (1978). A pre-requisite for initiation of these mechanisms is that sea level overtop the protecting beach. Normal summer storms blowing from northeasterly directions result in lower sea levels, exposure of the upper part of the 2m bench with waves breaking some distance from the bluffs. The formation of a thermo-erosional niche therefore is most commonly seen with westerly winds raising sealevel in the Beaufort Sea, and particularly with storm surges (Reimnitz and Maurer, 1979). Storm surges are rare and yet bluff erosion probably contributes the largest amounts of sediment to the sea during these short periods. At these times sediment transport is opposite to the long-term westward movement (Reimnitz and Maurer, 1979). The highest rates of thermo-erosion associated with niche development occur in areas of fine grained, ice rich coastal plain deposits widespread in the western third of the study area. In these areas sparsity of sand and gravel in eroded bluff material does not even permit the formation of beaches (fig. 5).

In the littoral zone and on the beaches along the Canadian arctic and Chukchi Sea coasts, seasonal variations in the depth to the upper surface of ice-bonded sand and gravel have been monitored (for example Harper et al., 1978). The bonded and presumably erosion resistant materials are generally less than a meter below the sediment surface both at the beach and at wading depths near the beach. According to theoretical calculations (Harper, et al., 1978, Taylor, 1980) maximum thaw rates of only 50 to 70 cm/day are indicated for storm conditions when released sediments can be removed at the same rate, thereby maintaining direct seawater contact with ice bonded sediments. Along the Beaufort coast much faster beach retreat rates have been documented. Harper, et al. (1978) speculated that here ice-bonding is not as widespread. However, permafrost studies, for example by Morack and Rogers (1981), and our own probing with rods indicate shallow ice bonding along the Beaufort Sea coast beaches and in the nearshore. Morack and Rogers (1981) demonstrated that the cores of rapidly migrating barrier islands (Reindeer and Cross Island, just east of study area) contain only sporadic bonding. According to jet drilling on these islands, the non-bonded materials seem to be brine pockets (Osterkamp, oral communication, 1985). Such sporadic ice-bonding suggests that the shoreline configuration of these islands during storm erosion should show irregularities corresponding with patchy ice bonding. We have weathered numerous storms behind these islands in our small vessels, and walked the islands without noting such irregularities in beach configuration. Theory, and measurements made elsewhere, therefore do not agree with our observations which suggest that ice bonding of beaches does not retard the transgression rate of the Beaufort Sea across the coastal plain.

The onset of winter, with decreasing water temperature, brings about conditions that have received very little study. In many polar regions the formation of an ice foot (Owens, 1982) is an important phenomenon. There are many forms and types of ice foot (Dionne, 1973), and a treatment here is not necessary. Once formed, an ice foot armors the beach, arrests erosion, and in many cases even results in beach accretion. The fact that sediment layers are interbedded with ice during the growth of the ice foot implies sediment movement from the foreshore onto the beach, and consequent steepening of the shoreface. In rare instances an ice foot does form along the Alaskan Beaufort Sea coast (Short, et al., 1974). However, our observations over many years during the fall, winter, and spring storms in the Beaufort Sea, with and without adequate fetch for wave generation, lead us to believe that ice foot is of little consequential to Beaufort Sea coastal processes. Stratified sediments on the beach face are ice bonded during cold storms, but erosion proceeds rapidly by ripping slabs of bonded sand and gravel from the beach (fig. 14C) and moving these in the swash zone, still intact, for some distance along the beach. During such times the back of the active beach generally is defined by a 1 to 1.5 m high vertical cliff of ice bonded sand and gravel (fig. 14C).

Littoral processes previously not documented for polar seas are those related to the formation of underwater ice (Martin, 1981) in the surf zone. Anchor ice, one form of underwater ice, is produced when water is so agitated at subfreezing temperatures that an ice cover can not form. The water becomes slightly supercooled and ice nucleates on the bed. This process is well documented in high latitude environments such as fresh water streams (Arden and Wigle, 1972, Tsang 1982, Osterkamp 1978). Our own observations, made during three different fall storms with 25 knot winds and air temperatures of -10°C , indicate that in marine waters less than 2 m deep the sediment becomes ice bonded. In one instance a 150 m diving traverse from the beach to 5 m water depth (Reindeer Island, October 1982) revealed ice-bonded sand and gravel interbedded with ice layers in a 30 m wide zone near shore. From the 2-m isobath seaward the seafloor was not ice-bonded but instead covered with pillow-size masses of ice (fig. 8). These ice-pillows consisted of an outer (10 cm thick) rind of fragile ice platelets, but were massive and sediment laden internally. These observations were made immediately after a three day storm and the bottom may well have been completely ice covered during the peak of the storm. The effects of this ice bonding and anchor ice formation on the coastal processes during fall storms is a matter of speculation. Our sketchy observations serve to demonstrate how little is actually known about arctic nearshore processes during times of severe fall weather; yet it is during this period that the greatest coastal changes occur.

A final littoral process to consider is the action of bulldozing of materials by ice from the littoral zone onto seaward facing beaches and barrier islands (Barnes, 1982; Kovacs, 1983). This process occurs mainly on those stretches of coast facing the open ocean and rarely in protected lagoons. The resulting ice piles normally contain sand and gravel that is left as hummocks after the ice melts (fig. 15). The processes were extremely active during the winter of 1982/83 based on a decade of observations in the study area. The chain of islands from Thetis through Cottle Island was marked by sand and gravel piles with average estimated volumes of at least a cubic meter per meter of shoreline. In one area a comparison of composition and distribution of the material shoved onto the beach by ice, and that of the nearshore sediment showed that the bulldozed material originated in large part from the shoreface out to 40 m seaward of the beach. While ice bulldozing during some years may help restore to the shoreface a part of what is lost by waves, currents, and other processes, we feel however, that its overall contribution is small.

METHODS

Retreat rates were obtained for the roughly 344 km of coastline by comparing two sets of charts at a scale of 1:50,000 covering the north coast of Alaska between Drew Pt. and Prudhoe Bay. This comparison is based on the shoreline, registered at mean lower low water by NOS. Some previous studies of coastal erosion focused on bluff retreat, which over short time periods is not always the same as shoreline retreat. For this reason our numbers locally differ from previously published ones, but overall show the same pattern.

The study area was divided into three major segments in order to present the overall coastline on the mapsheet at the desired resolution. Figure 21 serves as a key to these three major coastal segments and the 15 subdivisions used in our calculations. The original C&GS charts (numbers 9466 through 9472) represent the coastline configuration in 1949. The new H.O. charts depict the coastline as mapped by the state of Alaska in 1980. The seaward extent of the eroding coastal zone considered in our calculations is the 2-m isobath. Since the bathymetry was not resurveyed but stems from the original 1949-52 charts, we simply shifted the position of the 2-m isobath (mapsheet) landward in tandem with the local bluff retreat. Bathymetry from the previously undefined small shallow basin, near the coast off sector 9, was delineated by our own surveys in 1980, and is the only exception.

A few small areas not covered by the above charts were interpreted by comparing the 1949 coastline on U.S.G.S. topographic maps with the 1980 data. The maps were brought to a common

scale and projection, and changes in the coastal configuration registered using the same methods applied elsewhere. Areas treated in this manner (southern part of sector 6, western and eastern borders of sectors 11, and central part of sector 14) are identified on the mapsheet.

For convenience of discussion, the coast is divided into 15 sectors based on morphologic and geologic similarities. To calculate sediment input from coastal erosion, each of these sectors is in turn divided into 500m long segments numbered from west to east along the coast. The segments are treated individually.

Generalized nearshore geometry

Quantitative estimates of the sediment introduced by coastal erosion are based on the application of a generalized nearshore geometry (fig. 22) for each 500 m segment. In this model geometry, segment length, bluff height, changes in shoreline position, and distance to the 2-m isobath are measured values; whereas the width, slope, and thickness of the offshore component, and the indicated secondary prism dimensions are calculated values. The general model geometry distinguishes between the two different sources of sediment released to the sea during coastal retreat: 1) The sediment contained in the bluffs between the 1949 and 1980 coastal outlines, and 2) the volume eroded offshore between the new and old nearshore profiles out to the 2-m isobath. For a few particular segments (~ 14% of those studied) alternative geometries were applied. These are described under "Special case geometries" (fig 24.). Tabulated in the Appendix are all measured and calculated values, and parameters assumed in determining the sediment contribution from each of the 500m segments comprising the 15 sectors.

Sediment yield from bluff erosion

To calculate the sediment contribution from bluff erosion we use the 30 year coastal retreat distance (assuming bluff and shoreline retreat in tandem), bluff height, and the ice content of the eroded material (figs. 22, 23). Because the topographic elevations presented on published maps generally are several meters too high (Lewellen, 1977) the bluff height used in our calculations are obtained from the field notes of D.M. Hopkins, and S. Rawlinson, Reimnitz, and Barnes. In determining percentage of excess ice for the coastal plain sediments we referred to a data compilation by Sellmann, et al., (1975), giving excess ice content versus depth below the tundra surface for coastal plain deposits of the Gubik Formation near Barrow, Alaska (fig. 23). The eroded bluff materials in sectors 7 through 15 are coarser grained than those near Barrow, and therefore our assumed ice percentages here are somewhat high. However, in the rapidly eroding sectors 1 through 6 the coastal plain deposits are very similar in lithology, and therefore presumably ice content, to those at Barrow. Sellmann, et al., (1975) assume an in situ after-thaw-settlement porosity of 35 to 40%, while we assume that marine dispersal of sediment results in deposits of only 30% porosity.

In progradational or accreting areas of the coast, we calculated volumes for above sealevel material assuming elevations of 20 cm and 40 cm for delta mud flats, and beaches and spits, respectively. The use of these particular values is based upon our estimates from field observations.

Sediment yield from offshore erosion

To calculate sediment contributions to the sea from the erosion of seafloor material between the shoreline and the 2-m isobath we assume that the slope of the seafloor in this area of the nearshore is in dynamic equilibrium and remains constant as the shoreline retreats. This assumption is based on our local marine surveying experience. The distance of a vessel from the coast and the corresponding water depths, at almost any location, match those on 30 year old published nautical charts. This coincidence, and serious questions concerning the maintenance of such an "equilibrium profile" are discussed in detail later using a site in the western portion of the study

area as an example.

Figure 21 shows schematically the geometry of the eroded offshore areas and how we normally calculated the resulting sediment volumes. We assume no excess ice for the reworked offshore layer, which generally is only 10 to 20 cm thick (see sector tabulations 1-15 in Appendix). Assigning excess ice percentages according to the graph in figure 23 for the submerged layer changes our total volume estimates by at most 10%.

Where the 2-m isobath is highly crenulated, we arbitrarily smoothed it for our measurements. In the previously uncharted area off sector 9, where published charts place the 2-m isobath at 11 to 14 km from shore, we attempt to reduce possible errors by introducing bathymetry delineated from our own surveys in 1980.

Special case geometries

There are several exceptions to the general approach outlined above. The primary differences lie in deviations from the idealized geometry to more closely approximate volumes for unique local configurations. In all of these instances the special case geometries applied are identified and keyed to the particular segments concerned (sector tabulations in Appendix and figure 24A-D).

In sector 14 (Simpson Lagoon), where maximum water depths are less than 2m, the offshore volume considered takes the form of a triangular prism of lagoon-floor material whose apex is at the deepest central point of the lagoon (fig. 24A). The geometry applied here assumes that as the coastline retreats, there is no corresponding shift of the offshore margin, and its depth remains constant.

Two of the remaining three exceptions to the general geometry depict settings in which the landward shift of a relatively steep nearshore profile results in the removal of a substantially thicker prism of offshore material. In one case (fig. 24B) the distance covered by the retreating coastline is greater than the distance measured from the shore to the position of the 2-m isobath. This situation is common in the Cape Halkett area (sectors 5 and 6). We believe that using the general model here might result in values that are excessive relative to our generally conservative estimates for the offshore sediment yield. The second such case occurs where onshore migration of a spit or barrier and accompanying shift of the adjacent nearshore profile likewise results in the removal of a very thick offshore prism (fig. 24C). Examples of these type areas are Pitt Point and Pogik Bay. In the Jones - Return Island chain (sector 15) we assumed no volume change for the sand and gravel barrier islands (tan colored) in fig. 20). Even at the large scale used in this study, we were unable to resolve net volume changes in these barrier islands, and treated them as migrational bodies. Their motion is westward, obliquely onshore, or longshore, thereby adding to the overall westward nearshore sediment transport, but not to the overall shelf sediment budget. Similarly for the Eskimo Islands (sector 7), which like the cores of certain members of the Jones islands presently are stationary coastal plain remnants, we were unable to resolve net changes in the overall volume. Here erosion of westerly exposed tundra bluffs appeared to be compensated by accretion on adjacent and leeward beaches and spits.

The last exception to the general model deals with areas of actively accreting or prograding shorelines. Here we assumed a seaward shift of the shoreface and offshore profile, with prograding mud flats and beaches at respective elevations of +20cm and +40cm (fig. 24D). In the overall summary of volumes and weights, the net gain calculated for these areas was subtracted to arrive at the final sediment yield.

RESULTS

For each of the 15 sectors a tabulation appears in the Appendix showing both measured and calculated values used to determine the sediment yield from coastal retreat. These appendices are identified by sector numbers, and are keyed to numbers in figure 21 on the mapsheet. Table 1 summarizes the results for the entire area.

The average rate of coastal retreat for the 344 km of coastline studied is 2.1 m/yr. That rate includes the large Colville River system, with 48 km of coastline advancing an average of 0.4 m/yr. Excluding the delta, the erosion rate is 2.5 m/yr. After subtracting excess ice from the eroded bluffs, we calculate the annual sediment contribution from coastal erosion at $1.2 \times 10^6 \text{ m}^3$. This number is the sum of the sediment yield from all segments divided by 30 years. Using the same approach we calculated the annual sediment contribution from offshore erosion at $1.3 \times 10^6 \text{ m}^3$. The total annual sediment yield from coastal erosion therefore is $2.5 \times 10^6 \text{ m}^3$. To help visualize the significance of this sediment volume one can pro-rate it for the Holocene period (10,000 yrs) and spread it over the present shelf area adjoining the study area ($15,500 \text{ km}^2$). The resulting sediment layer would be 1.6 m thick. As discussed below, however, the offshore erosion associated with the present transgression can not be restricted to coastal waters of less than 2 m deep. The inner and midshelf is a surface of erosion, and the resulting sediment yield may be many times larger than we calculated.

Table 2 lists available sediment textures for coastal plain deposits exposed in bluffs. Christie Point (155° , $35'W$) and Tigvariak Island (147° , $15'W$) lie outside of the study area. The former is representative of the fine-grained deposits in sectors 1 through 6. The latter was included as an abnormally coarse grained section, as far as we know without counterparts in the study area. Only the data from Rawlinson gives information on the amount of organic matter contained in bluffs. But the 40 % he obtained from his extensive work around Simpson Lagoon probably is roughly representative for the entire region.

DISCUSSION

Regional patterns in erosion rates

There are large regional variations from the 2.1 m/yr average calculated for the 30 year period. Extremes range from an average 30 year retreat rate of 18 m/yr near Cape Halkett, to an average 30 year accretion rate of 20 m/yr near the active mouths of the Colville drainage system (mapsheet). There is a pronounced disparity in erosion rates between the western and eastern parts of the study area. The western portion is entirely composed of fine grained coastal plain deposits extending north from the Pelukian beachline (fig. 26). Retreat rates of bluffs here (sectors 1-6, but exclusive of Pogik bay with its unique setting), average 5.4m/yr. The remaining part of the study area lies east and to the south of the Pelukian beachline where coarser grained materials make up the bluffs. The average retreat rate for this section of coastline, exclusive of the Colville River Delta sector is 1.4 m/yr.

Long term changes in the coastal configuration are dependent on a combination of various climatic and oceanographic factors, as well as on the composition and geometry of the coastal plain transgressed. Severe short-term episodes of coastal erosion may locally play a significant role in the overall evolution of the coastline. An example is the 30 m of bluff retreat on Pingok Island experienced during one season. Most of this retreat occurred during a single storm event of several days duration (Short, 1973). During intervening years bluffs may locally appear entirely stabilized.

An understanding of regional differences in erosion rates in terms of geologic and oceanographic setting, would allow reconstruction of past shorelines, and a prediction of future trends in coastal evolution. Certain factors known to influence the erosion rates will be discussed.

Vertical movement of the earth crust is important in some parts of Alaska for coastal evolution, and will be analyzed first for the study area. The consistent altitude (7 m \pm 3 m) of the Pelukian shoreline from Barrow to the Colville River (Hopkins and Carter, 1980) are strong evidence that that stretch of the coast has been stable for the last 120,000 years. Thus Dease Inlet and Smith Bay, two of northern Alaska's most pronounced embayments, are not the result of differential vertical motion during that time period. According to Hopkins and Hartz (1978) the coastal plain deposits cropping out in the Jones Islands may also be Pelukian beach deposits. If true, the Pelukian beach deposits extend at a uniform level through the entire study area, except for a gap in eastern Harrison Bay. From our seismic records of the region, from industry borehole data, and from onland studies of the Quaternary geology (David Carter, oral communication, 1985), there is no evidence for Holocene subsidence of Harrison Bay.

Mean sealevels for the summer months from 1975 to 1984, measured by the U.S. National Ocean Survey at the east end of sector 14 are shown in figure 25. The best fit line for that data indicates a sealevel rise of 2 cm/yr or 2 m/100yrs. This is much higher than the 0.1 to 0.15 m/100yr worldwide sealevel rise and therefore suggests subsidence of that area. The configuration of shallow subbottom seismic reflectors in the region, in particular that of the Post-Pelukian unconformity offshore, does not support local subsidence. Furthermore, the modern coastal retreat rates in the area of the tide gauge are among the lowest of the entire study area. Thus we can find no support for the 9 yr sealevel trend shown by summer tidal data. All information available to us therefore suggests that irregularities in the coastline of the study area are not produced by differential vertical crustal motion during Holocene time.

Bluff height is one of the dominant factors controlling rates of erosion (Owens, et al., 1980). In areas of high bluffs and accordingly large sediment volumes the marine energy in some cases simply is inadequate to remove material at the same rate at which it is made available by melting. Areas that lack bluffs, as in figure 6, on the other hand are quickly inundated due to the extremely large amounts of ice in the upper 2 m of coastal plain deposits and the resulting thaw collapse. Here little lateral transport of sediment, or 'marine energy', is required to inundate the coastal plain. High bluffs along the Chukchi coast are partly responsible for the much lower erosion rates there than along the Beaufort Sea coast (Harper, 1978). Similarly, high bluffs in the Kogru River area are probably in part responsible for the lower erosion rates there than at Cape Halkett; although in this case the degree and direction of exposure and especially bluff lithology are perhaps the dominant factors.

The presence or absence of a beach, and its volume, strongly affect the coastal retreat process. Broad and high beaches are rarely overtopped by the sea, reducing thermal processes to ineffective atmospheric summer warming. One such area is the north coast of Pingok Island, where for reasons not well understood the beach broadened, even advanced, during the study period, yet the bluff continued to retreat. Because this study compares shorelines, while others may have considered the changes in the bluffline only, our erosion rates may differ from previously published values. The Pingok Island retreat rates shown in figure 32 are from Naidu (1984), and serve as example.

Variation in coastal plain composition (sediment grainsize) is an extremely important parameter. Coastal plain deposits containing pebbles and cobbles in a sandy matrix erode much slower than those composed mostly of silt and clay which have higher ice contents (Hopkins and Hartz, 1978). Areas with fine grained coastal plain deposits are also marked by a lack of protective beaches (fig. 5), due to a scarcity of sand and gravel size particles. The importance of grainsize is evidenced by the dramatic differences in coastal retreat rates between the eastern and western portions of the study area. From Oliktok Point eastward, where the coastal plain is composed of a series of coalescing alluvial and glacial outwash fans extending northward from the Brooks Range (Hopkins and Hartz, 1978); retreat rates are nearly an order of magnitude less than in the area to the northwest between Cape Halkett and Drew Point north of the Pelukian barrier chain (fig. 26) where bluffs are composed of marine mud (Carter and Robinson, 1980). These differences are

partly responsible for the more stable coasts in sectors 12 through 14 (1.3 m/yr) than those of sectors 1 through 6 (5.4 m/yr). The coarse Pelukian beach deposits north of Kogru River (sector 7), and exposed to the east in a number of the Jones Islands in form of high tundra-covered coastal plain remnants (fig. 18, and 20) (Hopkins and Hartz, 1978) are more resistant to erosion and control coastline evolution. Thus, the rapidly retreating promontory between Cape Halkett and Drew Point will likely stabilize at the ancient Pelukian barrier chain on the north shore of Teshekpuk Lake (fig. 26) in a few thousand years.

Degree and direction of exposure to the various climatic and oceanographic processes affect erosion rates. Open water conditions with waves and currents are needed to remove the materials introduced by bluff erosion. Simpson Lagoon is ice free for a greater part of the summer than the "open ocean" waters north of the Jones Islands (see typical ice distribution in fig. 19). The increased fetch in lagoons affords greater potential for erosive processes and consequently retreat rates in the lee of these islands are commonly higher than on the ocean-facing side (sector 15). Water temperature also affects erosion rates, partly owing to more effective niche development, and partly due to the extended open water season near river mouths. The coastal plain remnants in that part of the Jones Islands chain equidistant from the warming effects of the Colville and Kuparuk Rivers may be testimony to this influence. Such old remnants may have long since disappeared in the islands directly off the Kuparuk River, leaving barriers composed only of a thick sand and gravel lag atop residual tundra cores. Cannon (1978) pointed out that southfacing bluffs, those exposed to the sun for the greater part of the day, erode faster than north-facing bluffs. An example of the results of this difference in orientation is partly reflected in the higher erosion rate of bluffs on the south side of Pingok Island. Reimnitz and Maurer (1979) pointed out that storm surges, and therefore westerly winds in general, should be those most effective in producing significantly elevated tide and wave conditions, and thought that for this reason westfacing promontories retreat faster than those facing east. The resulting pattern, as best exemplified by the coastal configuration and retreat rates in sectors 13 and 14, is indicative of processes acting in a direction contrary to those responsible for the westward orientation of the small coastal spits trailing off the mainland promontories. This pattern however does not hold elsewhere in the study area.

Formation of embayments and lagoons by thermal collapse

Wiseman, et al. (1973) showed how thermal collapse of lakes breached by the transgressing sea results in embayments and lagoons (fig. 27). They envisioned a 4 phase evolution beginning with an area of large lakes similar to the Cape Halkett region. The coalescence of such lakes and the breaching and inundation by marine waters to form Kogru River type inlets is their second phase. This is followed by a widening of the inlet, and eventual stranding of coastal plain remnants to form an island-protected lagoon setting similar to that of Simpson Lagoon, as phase 3. The scenario is concluded by citing Leffingwell Lagoon (east of study area) as an example of maturity in phase 4. Reimnitz and Maurer (1979) have pointed out problems with this model, presenting Kogru River and Prudhoe Bay as examples. The lakes in these two regions are currently perched several meters above sealevel. Thus the anticipated amounts of thermal collapse of existing lake beds without subsequent deepening by erosion, could not create the 3 to 4 m water depths found in the two embayments. Also, enlarging the types of lakes found north of Teshekpuk Lake (fig. 26) as in phase two of Wiseman, et al. (1973) would result in water bodies oriented at right angles to the existing major embayments and lagoons we are trying to explain.

The lakes deeper than 2 m in the area north of Teshekpuk can be recognized by their persisting seasonal ice cover in figure 20 (Sellmann, et.al, 1975). Figure 26 indicates actual lake depths according to Holmquist (1978), C. Sloan, USGS (oral communication, 1980) and J. Helmericks, bush pilot (oral communication, 1984). The figure also shows three lakes that have been recently breached by the advancing sea to form very shallow NW-SE oriented embayments. Pogik Bay is one such embayment. The 2-m isobath, perhaps marking the northern part of this former lake basin, juts seaward by about a kilometer from the general trend of that isobath on

either side (see sector 4, Sheet 1). Thus the lake basin is a submerged promontory, more resistant to erosion than the surrounding terrain. Perhaps this can be attributed to the former existence of a deep lake underlain by a thaw bulb lacking excess ice. Upon breaching and inundation such lake bed would be dense and stable, and therefore not subject to further thermal collapse. A similar setting and evolution is described by Tomirdiaro (1975) for a cape in the East Siberian Sea. The cape marks a deep lake basin breached by the transgressing sea. Pogik Bay, however, is generally too shallow for use by even light float planes. The resistance to erosion here may alternatively be due to a thick accumulation of fibrous organic matter on the former lake bed.

The NE coast of present Cape Halkett may mark the west shore of a former large lake breached about 200 years ago. According to Leffingwell (1919, p.170), Dease and Simpson in 1837 mention a passage inside of a tundra-covered island which they named as the original Cape Halkett. Some 19th century charts (for example H.O. Chart no. 68, 1893 edition) show this island elongated parallel to the regional trend of lake axes. On figure 26 we stippled the outline of this island. The last tundra remnants of the island disappeared by about 1945, and in 1952 it was charted as a shoal (sheet 7991). The water depth over the former lake between the cape and the shoal is now less than 2 m.

Thermal collapse resulting in the development of coastal sediment sinks

According to our tabulations the sediment contribution from erosion in the offshore is slightly larger than that from the onshore. But the absolute reliability of the calculated values for this contribution is questionable due to the possibility of thermal collapse in the offshore zone. Harper (1978) in fact stated that "thaw subsidence causes a continual steepening of the offshore profile and provides a sediment sink for eroded sediments." In the following section we will analyze the Russian studies from the Laptev and East Siberian Seas commonly referred to in western literature (e.g. National Research Council, Marine Board, 1982) and then an example profile from our study area for evidence on thermal collapse.

Example from the East Siberian Sea

Russian workers have attributed the most important role in the shaping of the arctic continental shelf profile to thermal processes. Thus Tomirdiaro (1975) states "The eastern Arctic seas are largely young Holocene bodies of water formed by thermo-abrasional processes; it is thermo-abrasion, and not the usual abrasion processes, that has formed the so-called Arctic continental-oceanic zone here in such a short time." His interpretation relies heavily on the marine studies reported on by Klyuyev (1965). The data Klyuyev presents are hydrographic surveys repeated over time intervals of 15 to 20 years, off coasts that are retreating as fast as the coast in sectors 1 through 6 in our study. One of these surveys repeated after 15 years (Fig. 28) suggests a maximum lowering of the seafloor by 0.6 to 0.7 m in the depth range from 2 to 4 m, or a shoreward shift of the 2, 4, and 6 m isobaths by 0.5 to 1.2 km. The seafloor lowering was least adjacent to the coast, and on the outer end of the profile at 6 to 7 m depth. Klyuyev claims that the possibility of errors in navigation or in sealevel datum were definitely excluded in these surveys. We note that the 0-m isobath, which should represent the shoreline, remained stationary while the bluff had retreated by 170 m.

Klyuyev (1965) apparently attributes the depth changes entirely to thermal collapse, and presents evidence that the upper surface of the ice bonded section is at or immediately below the seafloor. The evidence he presents also can be interpreted differently. He reports that short cores may contain several millimeter long ice crystals. We have observed that small ice crystals form in fine grained sediments during fall storms, triggered by a rise in water salinity and a drop in water temperature to slightly below its freezing point. The sediment interstitial water still retains a slightly lower salinity acquired from summer river flow. The ice platelets seem to decay within a month into winter. He also reports ice in sediments and bonded sediments normally submerged areas exposed during strong winds. Ice bonded sediments in the Alaskan Arctic are also near the

surface on the 2m bench, where the fast ice rests on the bottom at winter's end. The thickness of the unbonded sediment layer in shallows, however, is not an indicator of the thickness of unbonded sediments offshore. He further cites as indirect confirmation of the existence of permafrost on the seafloor the following fact: "Vessels drift during a storm even with two anchors. The anchors slip over the solid bottom, and when the depth is slight a characteristic knocking can be heard." The bottom is not rocky where these observations were made. Such observations have also been made during fall storms in the Alaskan Arctic (Jim Adams, tug boat operator, oral communication, 1984). Our own work has shown that shallow water sand and coarser deposits during freeze-up storms become ice bonded and form anchor ice, as discussed earlier. Ice bonding, however, apparently forms only a surface crust, which disappears after the ocean has a new ice canopy. The annual formation of a seafloor crust can not result in net thermal collapse. The principal evidence for submarine thermal settlement brought forth by Klyuyev is the presence in the Laptev and East Siberian Seas of wedge-shaped depressions with peaked flanking ridges, which he interprets to be thermokarst features, resulting mainly from the melting of ice wedges. These are subdued in shallow waters, become best defined with increasing water depth (15 to 20 m), and are found seaward to 50 m water depth. This distribution pattern, with better preservation at increased water depth where sediments are more cohesive than on the inner shelf, and also the shapes of the features in fathograms, match exactly those of ice gouges on the Beaufort Sea shelf (Reimnitz and Barnes, 1974; Barnes, et al., 1984). The features are much too large (120 m wide) to be produced from the melting of ice wedges (* There is a large discrepancy between the 8 and even 12 m depression depth he quotes, and the maximum 5 m we measure from his figures). Lastly we note that thaw settlement in the coastal zone should result in the trapping of most sediments introduced. There should be little chance for sediment sorting, and underlying ice-bonded materials become buried by sedimentary accumulations. Yet the local bluffs introduce silt and clay-size materials, while offshore deposits are sandy. To us this indicates that mechanical, rather than pure thermal energy is at work winnowing the sediments introduced, that steep-sided depressions with flanking ridges are short-lived, and that the sedimentary environment is not unlike that of the Beaufort Sea.

Analysis of a North Slope profile

The following is an analysis of a coastal plain/continental shelf profile in the most dynamic region near Cape Halkett, to shed light on this question of offshore thermal collapse. Figure 29 is the overall profile compiled from published topographic maps and charts. A line on figure 26 indicates the precise location and trend of the profile. This particular line was chosen as an onshore continuation of an offshore profile which we have re-surveyed repeatedly for monitoring the rate of ice gouging from 1977 through 1980.

The coastal plain from the beach for a distance of 35 km inland has slightly undulating relief ranging between 5 and 12 meters above sea level. The last 5 km to the beach are marked by generally decreasing elevations, with a general slope that matches that of the seafloor for a few kilometers onto the continental shelf. The coastal zone is a pronounced niche in this profile, as amplified in figures 29B, 30A and B, and 31.

Unfavorable geometry of the shore stations with respect to the inshore end of the survey line (fig. 26) introduces possible north-south position errors of plus or minus 23 m between our own surveys. The western shore station is located at the corner of the hut at Esook (fig. 5), which has not been surveyed accurately. Thus there is an additional unknown error that affects the comparison between the 1950 and 1980 profiles. Our fathograms show slight local depth differences from one season to another during the 1977 to 1980 interval. But in view of the possible position errors, the overall bottom profiles are similar enough to be shown as a single solid line in figure 29B. This line is relative to a sealevel average for all survey periods, and has a likely error of 20 cm relative to the true datum. Our surveys stop at the bar marking the seaward edge of the 2m bench; the missing part of the profile from there to the beach is shown as a straight line. The dotted line in figure 29B is taken from a dense set of soundings made by the U.S. Coast and Geodetic

Survey in 1952.

The 30 year comparison of the inner shelf bottom profile shown in figure 29B suggests slight buildup (5-20 cm) at a distance of 5 to 10 km from the coast, and deepening (10 cm) in the first kilometer seaward of the 2m bench. This comparison also suggests that the seaward edge of the 2m bench maintained its position, while the coastline retreated. This is in conflict with the model we used for calculating sediment input by erosion. We have no data on any depth changes across the 2m bench, from where according to our methods and calculations the major part of the sediment budget is derived. The suggested widening of the 2m bench at this site during the last 30 years should be verified by increased navigational accuracy. But in the meanwhile an analysis of the offshore extension of the profile in light of the extremely rapid transgression is informative.

Figure 29B shows the shallowest seismic sub-bottom reflector below the shelf surface, as delineated by a 7 kHz profiling system used in conjunction with the depth recorder. This reflector is characterized by jagged relief of 2 to 3 m amplitude, indicated here schematically. The reflector is smooth only across the 2 m high, 500 m wide mound at 4.5 km from the coast.

In our Beaufort Sea geophysical studies we have generally taken the shallowest, continuous, sub-bottom reflector to represent the base of Holocene marine sediments, for reasons discussed by Reimnitz, et al. (1982). In numerous instances this interpretation has been confirmed by coring and other work. In the area of Cape Halkett however we have no such ground truth. If we assume this reflector is the base of the Holocene as elsewhere, then it may mark the former land surface, having been slightly modified by the bevelling action of the transgressing sea, which reworks just the upper few meters of coastal plain deposits. As the transgression proceeds, material below sealevel may for a time experience additional thaw collapse, and this may explain the different slope of the inshore 5 km of the seafloor and sub-bottom reflector. As thaw settlement is complete and all material reaches equilibrium with the thermal regime, the slope of the seafloor flattens out at an attitude parallel the slope of the old tundra surface. Following this line of reasoning the vertical distance separating the trace of the old tundra surface bevelled to sealevel and the position of the first sub-bottom reflector is explained by 8 m of erosion and thaw settlement, followed by re-deposition of 4 m of bluff and nearshore material. This hypothesis is illustrated in figure 30A and is shown to be unlikely later on.

The jagged sub-bottom reflector is characteristic of several extensive regions in the Beaufort Sea. In one such area industry soil borings showed the reflector to conform to the top of ice bonded sediments. At two sites several km west of our profile Harrison and Osterkamp (1981) investigated the depth to ice bonded permafrost. At 2.7 m and at 5.5 m water depth, the first ice was penetrated 4 and 5 m, respectively, below the seafloor. At the latter hole, the phase change from partial to solid bonding occurs between 5 and 7 m, and Osterkamp believes that the boundary from which seismic energy is reflected should be very irregular under these conditions (oral communication, 1984). Alternatively then the sub-bottom reflector in figures 29B and 30A may more likely mark the upper surface of bonded subsea permafrost. From the point where the reflector terminates in shallow water, it probably rises beneath the 2m bench, to conform to the seafloor from there to the beach, and rise sharply to the land surface at that point. If so, this reflector can not also be the former coastal plain surface, or the interface between older and Holocene sediments.

Figure 29A shows where the inner shelf profile would have been 1000 years before the present, assuming the maintenance of a profile of dynamic equilibrium. Even if the seafloor slope was much steeper at that time, this reconstruction implies a large wedge of material unaccounted for in our calculations of sediment removed during transgression. Our tabulations account only for the hachured portion of this cross section. In figure 30B we indicate how much of the implied missing wedge can be reasonably attributed to thaw settlement. We again use data from Sellmann, et al. (1975), and assume that sediments in situ retain a porosity of 40% after thaw collapse. Sellmann's data from the Barrow area shows that most excess ice, and therefore thaw

settlement, occurs in the upper 7 m of the coastal plain. We apply that data to two hypothetical cases, where both assume a constant sealevel. In the first case the coastal plain extended seaward horizontally at a level 3 m above the present sea, and has been removed to the -2 m level by erosion and deposited elsewhere. This slab is shown in a stippled pattern. The thickness of the line at the base of this slab represents the amount of thaw settlement possible for that erosion surface (about 5 cm). In the second case the old tundra surface intersects sealevel 3 km from the present shore, and again is truncated down to the -2 m level. We can only make reasonable estimates of thaw settlement for this erosion surface from the edge of the 2m bench to the point where the coastal plain dips below sealevel. The possible thaw settlement is indicated as a wedge, with a maximum thickness of 39 cm at a point where today's water depth is 7.5 m. At this point the discrepancy between the eroded slab we account for in our sediment yield calculations plus thaw settlement and the actual seafloor is about 5 m. Using available data the maximum thaw settlement that could have occurred anywhere along this profile is about 1.5 m.

Although we do not know the distribution of excess ice in the offshore, our analysis of the profile strongly suggests that the niche in the coastal zone must be due either to a) erosion by lateral transport through a combination of processes involving ice, waves and currents; or b) was produced over a long time period in a somehow different setting, in which the coast was stable. We rule out the latter, as analyses of temperature profiles in 5 boreholes offshore from Pitt Point (sector 2) indicate a retreat rate of several meters per year for the last 1000 years (Harrison and Osterkamp, 1981). Furthermore, Lachenbruch (1985) states "the absence of a thermal disturbance in coastal wells along the Beaufort Sea implies the shoreline has been transgressing rapidly".

The transgression is rapid along the entire Beaufort Sea coast from Barrow to the Mackenzie Delta in Canada (Hopkins and Hartz, 1978). The profile discussed above is not unusual for this coast, except off the two largest rivers the Colville and the Mackenzie. The bluff retreat is not associated with the formation of a platform near sealevel. This implies that the entire inner shelf should be an erosional surface, with possibly several tens of meters removed since the transgression.

There is indeed strong evidence that much of the Beaufort Sea inner shelf is an erosional unconformity. Reimnitz et. al. (1982) showed a sparsity of Holocene marine sediments for the region between 146°W and the Canadian border, and presented seismic evidence indicating that the inner and mid shelf surface truncates older strata. Isopach maps of Holocene sediments prepared since show that such materials are restricted to bays and lagoons in that region. Similarly, the inner shelf surface between 146°W and the present study area, from the island chains to about 30 m water depth, truncates seaward dipping older strata (on-going work by Steve Wolf and the authors). These findings are supported by studies of over 20 boreholes in that area. Over-consolidated silt and clay cover much of the Alaskan Beaufort Sea shelf. Lee and Winters (in press) studied the consolidation properties and mechanisms for surficial sediments and conclude that subaerial freezing during periods of lowered sea level was probably the principal cause. Only the lagoons contain local accumulations of soft Holocene marine sediments. Analysis of seismic records from there to Harrison Bay has not been completed, but the data indicate a similar setting.

Vertical shelf erosion by a shifting "equilibrium profile"

In seas not dominated by ice, the inner shelf apparently maintains a profile of dynamic equilibrium, by some referred to as "Bruun's Rule" (Bruun, 1962; Schwartz, 1967; Swift, 1968; and Rosen, 1978). Winant, et al. (1975) show that seasonal changes in the profile across the beach and out to 10 m water depth can be described using empirical eigenfunctions. While the year round presence of drifting pack strongly affects processes and very likely also the shape of the profile, we can nevertheless assume that the profile is maintained and shifted landward as the sea transgresses. Let us consider the implications of a dynamic equilibrium profile through the last thousand years for the Cape Halkett area.

As depicted in figure 29A, sea level likely was constant while the coast retreated about 10 km. This reconstruction has two important implications: 1) the amount of sediment supplied to the sea by erosion is increased by at least a factor of four over that calculated from bluff and shallow nearshore erosion alone, and 2) we can calculate vertical erosion rates for any point on the inner shelf. The latter is shown in figure 31. The length of arrows along the profile in this figure indicate the depth to which erosion would lower specific points on the seafloor during the next 100 years by a simple landward shift of our assumed "equilibrium profile". The scale to the right of the profile shows the expected vertical erosion over time for a point originating on the tundra surface. While the arrows along the profile will not serve as actual measures of seafloor erosion to be expected in the design of buried offshore pipelines, they do indicate a situation of considerable import to the development of the offshore oil fields. Dunton et. al. (1982) presented supporting evidence for vertical erosion at 6 m depth in the sheltered waters of Stefansson Sound, directly off the Sagavanirktok River. This ongoing erosion resulted in the Boulder Patch as a modern lag deposit.

Total sediment yield from rivers and from coastal erosion

To obtain the sediment yield for that portion of the North Slope feeding the shelf within our study area, we must first evaluate what is known about the river input to the sea. Milliman and Meade (1983), using 5.8 millions tons as the annual suspended sediment load of the Colville River (Arnborg, et al., 1967), with a drainage basin of 50,000 km², estimate northern Alaska's sediment supply from rivers at 120 tons/km²/yr. For the following reasons we believe that number is an order of magnitude too high: Vast regions in the Eurasian Arctic with similar settings as that of the Colville River drainage area yield 8 tons/km²/yr according to the compilations by Milliman and Meade (1983). They use that same number as an estimate for northeastern Canada. The Mackenzie drainage basin yields only 55 tons/km²/year (Milliman and Meade, 1983). The Babage River (between the Mackenzie and the Alaskan border) according to two years of measurements by Forbes (1981) yields 42 tons/km²/yr. The yield for these two rivers should be much higher than that of the flat Colville River drainage area. The Sagavanirktok River immediately east of our study area (draining 14,500 km²) according to our own sketchy measurements yields about 5 tons/km²/yr, and according to one summer of stream gauging by NORTEC yields 7.4 tons/km²/yr (R.P. Britch, written communication, 1984). Even the Sagavanirktok River, judging by its steeper gradient and braided nature, should have a higher sediment yield per unit area than the Colville River.

In view of the above considerations, we estimate 10 tons/km²/yr as the sediment yield from 74,000 km² drainage areas adjoining the coastal sector studied here (fig. 1). Upland sources accordingly yield 740,000 tons of sediment per year. This compares to about 5 million tons per year, contributed by coastal erosion. Previous studies estimated that streams supply four times more sediment to the Beaufort Sea than coastal erosion (Owen, et al., 1980). According to our own calculations the sediment yield from coastal erosion is seven times higher than that from streams, and we believe that factor is very conservative.

Inner Shelf Erosion a Major Sediment Contributor

Based on the geometry assumed in our study, the thickness of the sediment layer removed between the shoreline and the 2-m isobath during the 30 year period of coastal retreat typically is less than 20 cm. In reality the layer very likely is many times thicker, and also extends seaward far beyond the 2m isobath. Thus the sediment yield resulting from the erosive transgression is many times larger than we calculated. If this is true, then the rate of coast transgression is influenced not only by the lithology of bluff materials, but by the lithology of sediments underlying the inner continental shelf. Some of these subsea deposits may find their way to the beaches, and in turn affect their lithologies.

From the above considerations it follows that the several meter thick blanket of Holocene marine sediments found locally on the actively eroding part of the profile represents sediment in transit, or in flux. Over large areas this layer is about as thick as the maximum ice gouge incision depth (Barnes, et al., 1984), or roughly one tenth of the water depth out to the 40-m isobath. Off certain deltas the layer is about as thick as the depth to which strudel scour reworks the section, or about 6 m (Reimnitz and Kempema, 1983). These processes excavate underlying, older sediments and admix them into the flux. The resulting layer may be viewed as a roto-till, or better "gouge-till" unit. These sea ice related, erosive processes explain why the surface sediments contain mixtures of modern Foraminifera together with iron-oxide stained, old forms that are outside of their depth range and habitat (Kristin A. McDougall, oral communications, 1984). The processes also explain why clay mineral suites in surface sediments, unlike patterns on other Alaskan shelf regions, do not reveal patterns that can be traced back to their continental source regions. The distribution of suites instead is patchy, and has been attributed to relict nature of surface sediments (Naidu and Mowatt, 1983). The materials probably are derived to a large extent from erosion of local sources on the shelf, and are incorporated into the surficial "gouge-till" unit.

Given the sediment input from coastal erosion and streams, and published estimates of littoral transport in the Beaufort Sea, one is led to attempt completing the sediment budget by considering the sinks. Placing the sediment budget within the constraints of the concept of a littoral cell, including sources, pathways, and sinks (e.g. Inman and Chamberlain, 1960; Inman and Brush, 1973) has proven useful in studies elsewhere. The concept requires a dominant source at one end, and a major sink somewhere off the other end of the cell. This concept seems to break down where the system is not dominated by a point source, as in our case. A really rather evenly distributed input from erosion of the Beaufort Sea coast far outweighs the riverine input. Average littoral transport is capable of passing about ten thousand tons past a point along the shore (e.g. Short, et al., 1974). The average sediment input resulting from coastal retreat is $7,300 \text{ m}^3/\text{km}$ of shoreline. As reported earlier, the above-sealevel part of the coastal plain in the study area is composed of about 50% sand with less than 1% of gravel, the material considered in littoral transport estimates. This implies that the littoral transport system at any specific point will choke from the sand introduced from only about 3 km of updrift coastline. This further implies that either the sediment sinks are closely spaced, or other transport agents than those considered at low latitudes dominate the arctic sedimentary environment.

A lack of sediment sinks on the exposed inner shelf, and the restricted occurrence of Holocene sediments within the shelter of certain lagoons, has already been discussed. Can the sediments collecting with the lagoons, and those contained within the islands chains, account for the sediment input to the Beaufort Sea over geologic time scales? We take a look at Simpson Lagoon in an attempt to shed light on that question. Crude calculations comparing the present volume of the lagoon with its sediment supply indicate the basin would fill to sealevel within several hundred years. That obviously is not occurring, and therefore the lagoon over long time spans can not accomodate the sediment introduced, but is by-passing large amounts of material. The fact that the lagoon is being enlarged by erosion greatly complicates any attempts to predict even its immediate future. The lower part of figure 32 views the development of Simpson Lagoon paleo-shorelines during the last five thousand years, as interpreted by Naidu, et al. (1984) from bluff retreat rates. We noted previously that measurements of bluff retreat rates over short time periods are not expected to parallel shoreline retreat rates exactly, and in this case do differ from our values. The upper part of figure 32 is a present day profile of the area, together with hypothetical profiles 1000 yrs ago and predicted for the year 3,000, based on the regional average erosion rate of 2 m/yr. This profile evolution is intended to depict a lagoon, rather than Simpson Lagoon specifically. The profile also shows the generalized upper surface of a thick underlying unit of massive gravel specific to Simpson Lagoon. We constructed this profile from 12 soil borings in the area, as shown.

The information contained in figure 32 leads to the following observations: Even during the last five thousand years, since worldwide sealevel rise reached its present position and the

transgression ended elsewhere, it continued at such a rapid rate in the arctic that lagoons must be considered as ephemeral features only. Thus even the modern deposits contained in arctic lagoon/barrier island systems can not serve as long term sediment sinks. These deposits are a flux, to be re-mobilized by the advancing sea within several thousand years. More importantly, the modern lagoon/barrier island morphology and deposits are only thin surficial features in the predicted deep-reaching profile evolution during two thousand years. This profile seaward of the islands apparently has cut a deep notch into the underlying fluvial gravel.

Since even the outer shelf is presently an area of sediment by-passing (Reimnitz, et. al., 1984), the ultimate depository should be the Arctic Basin floor. While deposition rates in the deep Arctic Ocean have in the past been thought to be very low, recent work by Sejrup, et al. (1984) suggests values many times higher.

Surficial sedimentary deposits of the coastal plain north of the Pelukian shoreline (fig. 26) are tentatively interpreted as inner shelf deposits laid down during the last marine transgression (Carter and Robinson, 1980). Similar interglacial units of up to 15 m thickness underly much of the present inner shelf, where they are being truncated by the current transgression. Thus the Holocene transgressive and erosional environment seems to contrast with depositional environments of past interglacial periods. One known difference between the last interglacial period and the present is that sealevel was 7 to 8 m higher than now. We feel that higher water level alone can not explain why marine sediments accreted in shallow water during past transgressions and were preserved. There is however a growing body of evidence indicating that the last interglacial transgression had warmer air and sea temperatures than today. This implies there was less sea ice. Thus Carter (1980) states the "straightness of a 250 km long barrier chain and presence of microfauna now endemic to the North Atlantic indicates that Pelukian deposits of northern Alaska formed at a time when the Beaufort Sea and channels between the Canadian Arctic islands were more open than now" (Carter, 1980). Also, studies of over 20 offshore boreholes suggest that marine deposits of Pelukian age were not disrupted by ice gouging (Peggy Smith, oral communication, 1984). Conditions during the last transgression, when glaciomarine sediments of the Flaxman Formation were deposited, are less clear. Carter (written communication, 1985) feels that Flaxman deposits may originate from a time when enormous volumes of floating glacial ice were produced by the rapid break-up of a large part of the Laurentide ice sheet. The presence of much glacial ice, and findings of fossil ribbon seal and gray whale very rarely found in the Beaufort Sea today, might also indicate warmer conditions, and possibly again less sea ice growth than at present.

Comparison with Gulf Coast erosion rates

May, et. al. (1983) compiled information on the erosion rates of U. S. shorelines. They state "the Gulf coast states have the distinction of having the most rapid average erosion rates (1.8 m/yr) on a national scale." The Texas coast is marked by lagoons bordering a flat coastal plain, and recent crustal stability. This coast, eroding at an average rate of 1.2 m/yr, in many respects has a setting similar to that of the North Slope. The Beaufort Sea coast retreats at a rate almost twice that high, and average rates in the Soviet Arctic seem to be still higher (Tomirdiario, 1975).

When considering the actual time frame in which dynamic nearshore processes act in the two different environments, a major discrepancy in erosion rates becomes evident. At lower latitudes the marine forces attacking the coasts are at work for 12 months of the year, while the arctic shoreline retreats only during three summer months. For the majority of the year, and including the period with the severest weather, the arctic shoreline is frozen and stable under a protective coat of snow and ice. Elsewhere during this period the greatest coastal damage is done. Using a common denominator then in our comparisons of Texas and North Slope erosion rates, we find that the latter is a minimum of 8 times higher. This raises the fundamental question: What mechanisms or forces make the arctic coastal environment more erosive than that of lower latitudes?

Some workers have attributed the high erosion rates, and even the characteristic shelf profile of the arctic largely to thermal processes. In this study we have shown that after the process of thermal collapse is complete, much mechanical energy is required to transport away large sediment volumes to account for the maintenance of the present shelf profile with coastal retreat.

Wave energy in the classical sense can not account for the rapid erosion of the coast and shelf. Published sediment transport estimates for the littoral zone do not account for the action of floating ice wallowing in a wave train along the shoreface. Reimnitz and Kempema (1982) have demonstrated the formation of large, irregular hydraulic bedforms resulting from the interaction of waves and currents with ice touching the seafloor to at least 10 m water depth. But net sediment transport has not been quantified. Computations of toe protection required around a hypothetical cone drilling structure under assumed wave and current conditions in the Arctic predict the erosion of gravel size sediment out to 20 m water depth (Kobayashi, 1981). The effects of ice keels in bottom contact or even barely skimming the sea bed without actually going aground should be similar. Thus sediment erosion from hydraulic processes as a result of flow interaction with ice keels probably extends far beyond the 20-m isobath. In two separate studies we have shown that bedload movement is rapid far beyond the surf zone. In one study bedload transport at $9 \text{ m}^3 \text{ yr}^{-1}$ was measured at a distance of about 4 km from shore (Reimnitz and Kempema, 1983). This was assumed shore-parallel, but may have an offshore component. In another study, involving repetitive surveys to monitor ice gouging rates in Harrison Bay, Barnes and Reimnitz (1979) report fall storms obliterated all gouges from the shore to 13 m water depth, at a distance of 15 km from land. Here also extensive sand movement occurred. The mechanism by which the sediments were moved are unclear, but we suspect that underwater ice formation (frazil and anchor ice) may play a role. Frazil ice formation during fall storms certainly is involved in the incorporation of large volumes of fine sediment into the seasonal ice canopy in some years Barnes, et al. (1982), Osterkamp and Gosink (1984). During the winters 1978 and 1979 the sediment-laden ice extended out to the stamukhi zone, with concentrations of 243 t/km^2 and 800 t/km^2 , respectively (Barnes, et al., 1982). According to rough calculations the area between the coast and the stamukhi zone, as mapped by Reimnitz, et al. (1978), covers $3,290 \text{ km}^2$ in the study region. Thus the ice canopy held $.79 \times 10^6$ tons in 1978, and 2.6×10^6 in 1979. In the first of the two winters the sediment was composed mainly of silt and clay, but sediment samples collected from the ice in 1979 contained up to 30 % sand. Sediment weights held by the winter ice canopy therefore are significant in terms of the overall sediment budget. However, since most of the sediment is released locally to the water column during the following summer melt, summer rafting of sediment introduced into the fast ice by fall storms can not account for all of the sediment eroded. During the fall storms and the actual production of frazil ice the inner shelf waters may be flowing at a rate of over two knots for several days. We believe this may be the time when most sediment is transported away from the region. But much work needs to be done, under conditions which man has not yet learned to cope with, before a basic understanding of arctic erosion and transport mechanisms can be achieved.

ACKNOWLEDGEMENTS

We received much information and help from S. Rawlinson in the initial stages of this study, and thank him for sharing his data. Personal insights of P. Sellmann broadened the scope of this investigation. His constructive criticism and review, together with those by D. Inman and D. Hopkins are gratefully acknowledged. L. Gaydos and W. Acevedo were instrumental in providing us with enhanced Landsat imagery for figure 20. J. Dailey helped us determine the vintage of data sets used in delineation of the coastline in the original base maps. A. Kovacs provided us with several photos of key localities in the study area. A. Campbell assisted in the preliminary gathering and reduction of data.

This study was funded in part by the Minerals Management Service through interagency agreement with the National Oceanic and Atmospheric Administration, as part of the Outer Continental Shelf Environmental Assessment Program.

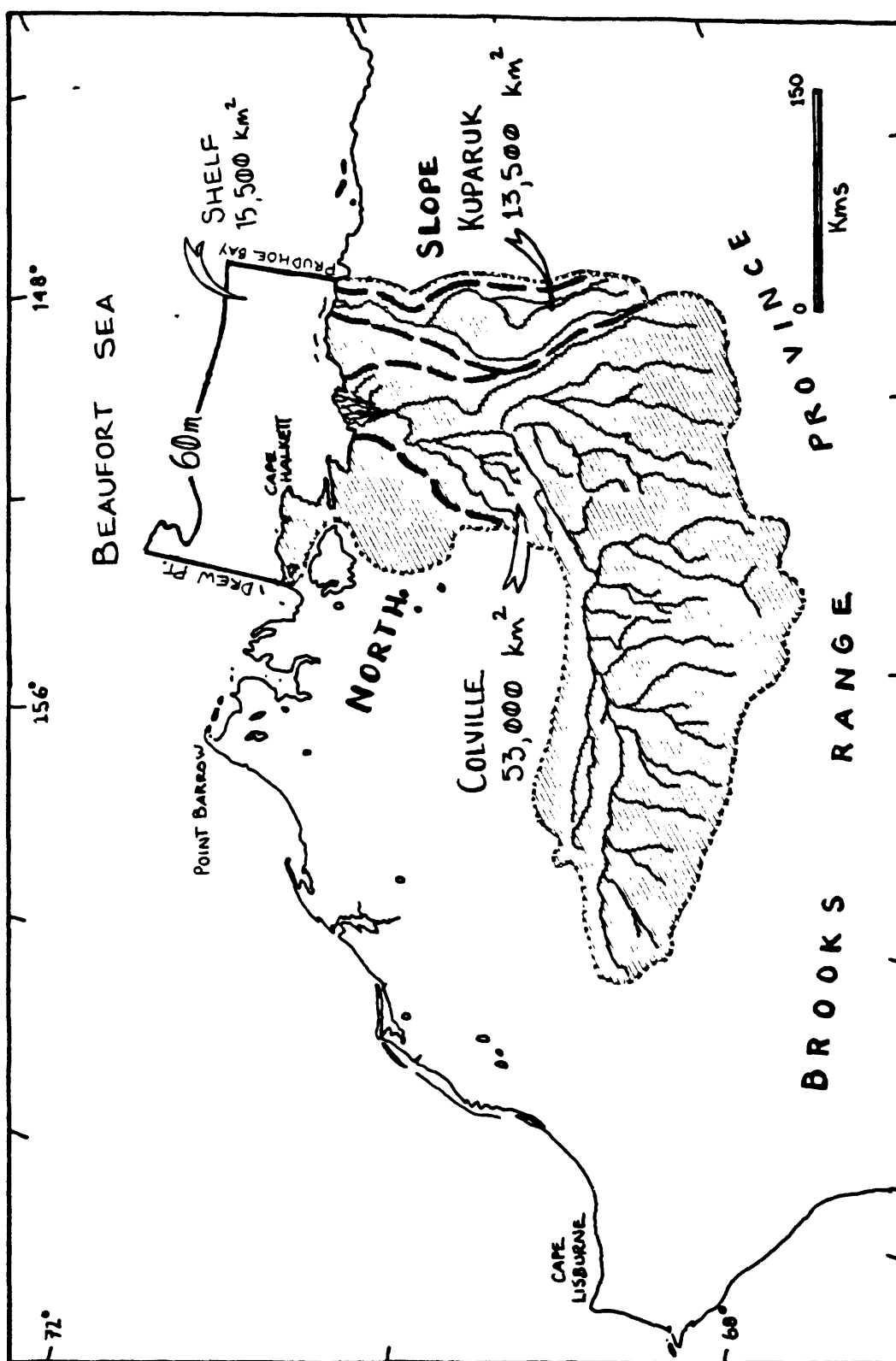


Figure 1. Map of Drainage and Shelf Areas considered in our study.

Table 1

SUMMARY OF ANNUAL SEDIMENT YIELD			
FROM COASTAL EROSION:			
Overall Erosion Rate = 2.1 m/yr			
without Colville Delta sector = 2.4 m/yr			
		Per Kilometer	Total
Bluffs	volumes =	3500m ³	1200000m ³
	weights =	6600tm	2300000tm
Offshore	volumes =	3800m ³	1300000m ³
	weights =	7200tm	2500000tm
Total	volumes =	7300m ³	2500000m ³
	weights =	13800tm	4700000tm
FROM RIVER INPUT:			
Combined Drainage Area		74000km ²	
Average Denudation Rate		50tm/km ²	
	volumes =	1950000m ³	
	weights =	3700000tm	

Table 2

CLASTIC COMPONENT OF BLUFFS				
Sample Location	Grain Size %			Reference
	gravel	sand	mud	
Oliktok Pt. & Kavearak Pt.	0	69	31	R. Lewellen 1973 writ. comm. (average of 2 smpls.)
*Simpson Lagoon	0	85	15	S. Rawlinson 1983 writ. comm. (average of 60 smpls.)
!# Tigvariak Isl.	2.6	62.9	34.5	Reimnitz & Barnes unpub. (average of 2 smpls.)
	2.5	61.9	35.6	
Atigaru Pt.	0	85	15	R. F. Black 1964
Drew Pt.	0	8	92	
Teshekpuk L.	0	42	58	
!Christie Pt.	0	32	68	

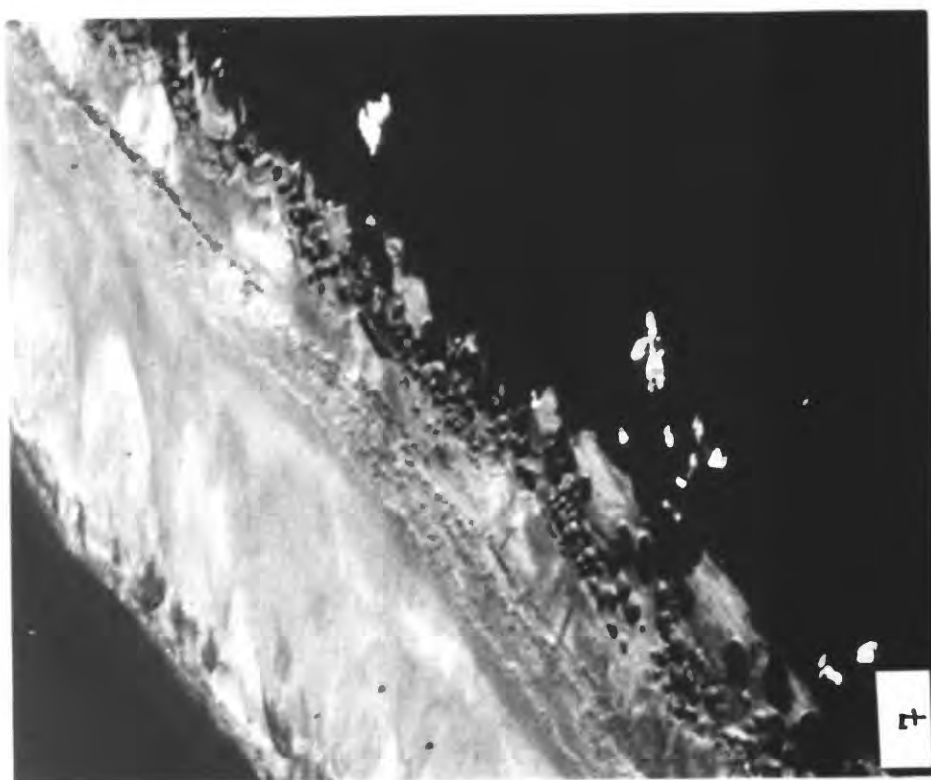
* organic component up to 41% of overall bluff composition

! chosen for its unusually rich accumulation of gravels

location outside of study area

- Figure 2. Slumping of 2 m bluff following formation of basal niche.
- Figure 3. June 20 photograph of Pogik Bay and flat, lake dotted coastal plain prior to breakup of fast-ice.
- Figure 4. Aerial photographs comparing the coastline at Esook in 1949 and 1981 demonstrating 410 m of bluff retreat. The near vertical arrows point to the same hut on the two photos (from Kovacs, 1983).
- Figure 5. Low altitude oblique photo of last remaining hut at Esook Trading Post (from Kovacs, 1983).
- Figure 6. Aerial photograph of a beach transgressing over low tundra with ice wedge polygons (from Kovacs, 1983).
- Figure 7. Low altitude oblique photo of seaward side of a barrier island showing ice-wallow relief.
- Figure 8. Pillows of anchor ice (underwater ice attached to submerged objects) found widespread in shallow coastal waters during freeze-up storms. The pillow in the foreground is 50cm across and attached to medium grained unfrozen sands at 5m water depths.
- Figure 9. Fresh exposure of a 2 m high coastal bluff cutting massive ice in longitudinal section.
- Figure 10. Cross section of ice wedge in cryoturbated sandy bluff (glove for scale).
- Figure 11. Erosional niche at the base of a high bluff in aeolian (dune) sands.
- Figure 12. Erosion of low, vegetated, inactive delta front.
- Figure 13. Silt flats on prograding part of delta.
- Figure 14. Thetis Island: A) gently sloping beach in 1979 after a winter of ice-override, note striated slope B) beach scarp on september 12, 1982 C) and on october 9, 1982 after fall storm.
- Figure 15. Gravel covered ice rubble pile.
- Figure 16. A) ice wallowing in surf zone, and B) the resulting relief.
- Figure 17. Low coastal plain marked by two storm surge lines.
- Figure 18. Freshly undercut 3 m high bluff.
- Figure 19. Typical summer conditions on seaward-facing beach.













19



083-010

Figure 20. Landsat image (august 1, 1976) of central study area showing:

- 1) typical summer ice distribution, restricting significant fetch to warm and sheltered waters, 2) absence of protecting barriers along Cape Halkett coast, where most sediment is introduced, 3) tundra-covered older surfaces (including numerous islands), versus recent, active, and barren surfaces (delta flats and barrier islands), 4) deep (over 2m) ice covered lakes versus shallow ones, and 5) sediment-laden waters around the stagnant Colville Delta.

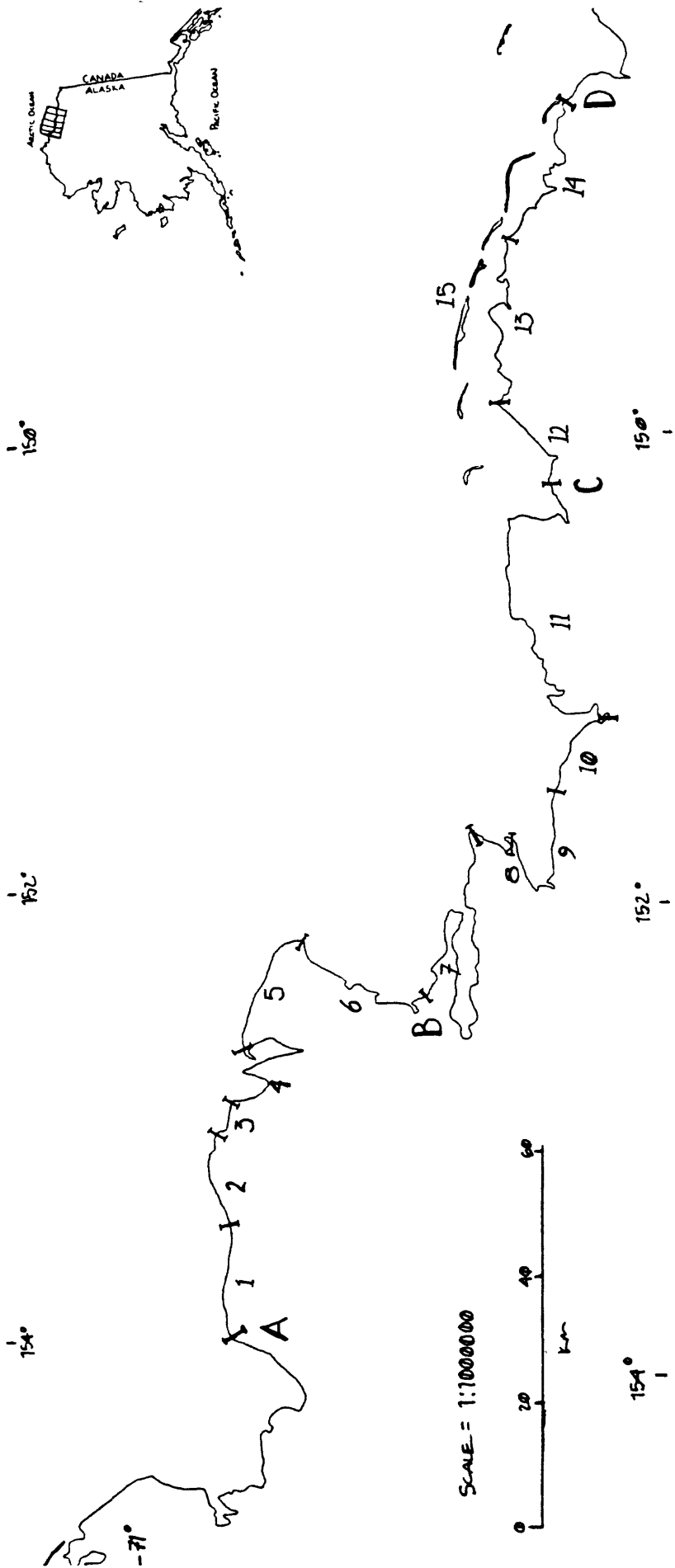
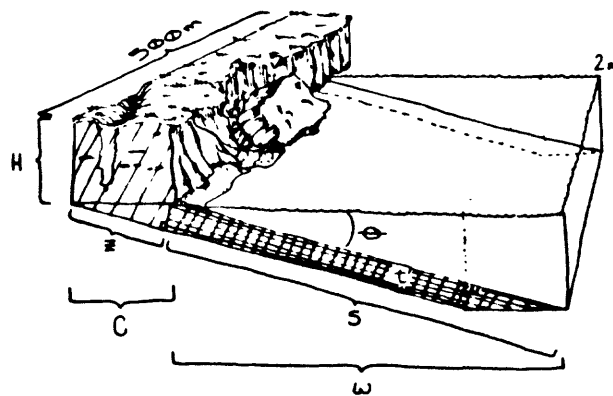


Figure 2.1. Index map for the 3 major coastal segments represented on this mapsheet, and for the 15 sectors for which calculations are tabulated in the appendix.



MEASURED PARAMETERS

500m segment length
H bluff height
C change +- in coastline
w distance to 2m isobath

CALCULATED PARAMETERS

Θ offshore slope = $(\arctan 2/w)$
s width of offshore polyhedron = $(2/\sin\Theta)$
t thickness of offshore polyhedron = $(C\sin\Theta)$
z secondary prism width = $(C/\cos\Theta)$

EQUATIONS

v_i (initial bluff volume) = $500(HC + 0.5zt)$
 v_1 (bluff volume - excess ice%) = $v_i - \text{excess ice\%}$
 v_2 (offshore polyhedron volume) = $500(st - 0.5zt)$
V (total volume input) = $v_1 + v_2$
T (total weight input in metric tonnes) = $1.89V$

Figure 22. General geometry used for volume calculations:

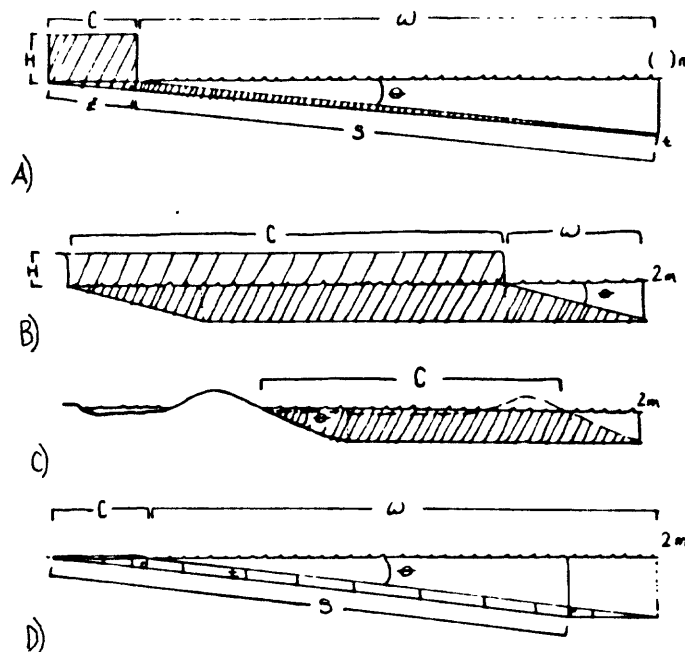


Figure 24. Special case geometries:

- A) where segment borders lagoon with a maximum depth < 2 m
 $v_i = 500(HC + 0.5zt)$, $v_1 = v_i - \text{excess ice\%}$, $v_2 = 0.5(500st)$
B) where $C > W$
 $v_i = 500HC$, $v_1 = v_i - \text{excess ice\%}$, $v_2 = 500C^2$
C) where barrier or spit shifted onshore
 $v_i = 0$, $v_1 = 0$, $v_2 = 500C^2$
D) where accretion has occurred
 $v_i = v_1 = +500HC$, $v_2 = +500st$

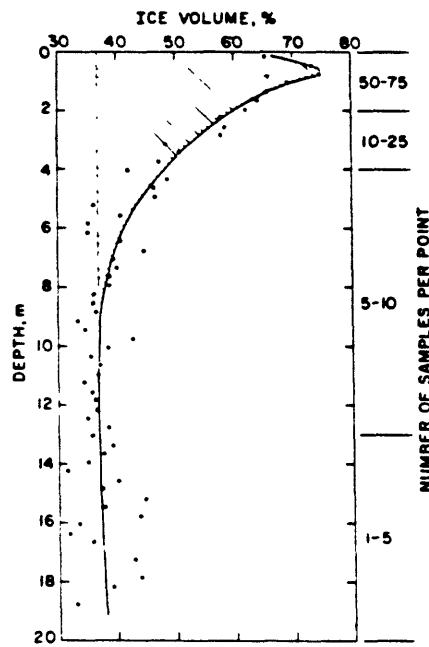


Figure 23 Graph of ice content versus depth below tundra surface (after Sellman et. al. 1975).

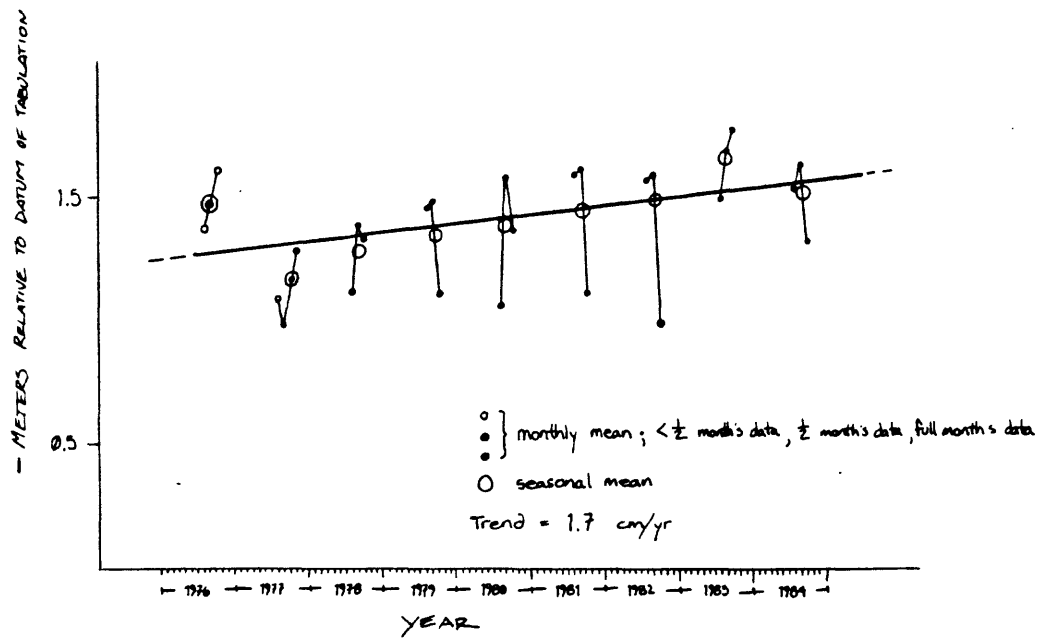


Figure 25 Graph of monthly (july, august, and september) mean and seasonal mean sea level measured at Prudhoe Bay West Dock - NOAA tide station #949-7649. Trend line represents least square fit to seasonal mean data. Note sea level usually peaks in august (spring floods) and decreases thereafter. (after Inman 1984)

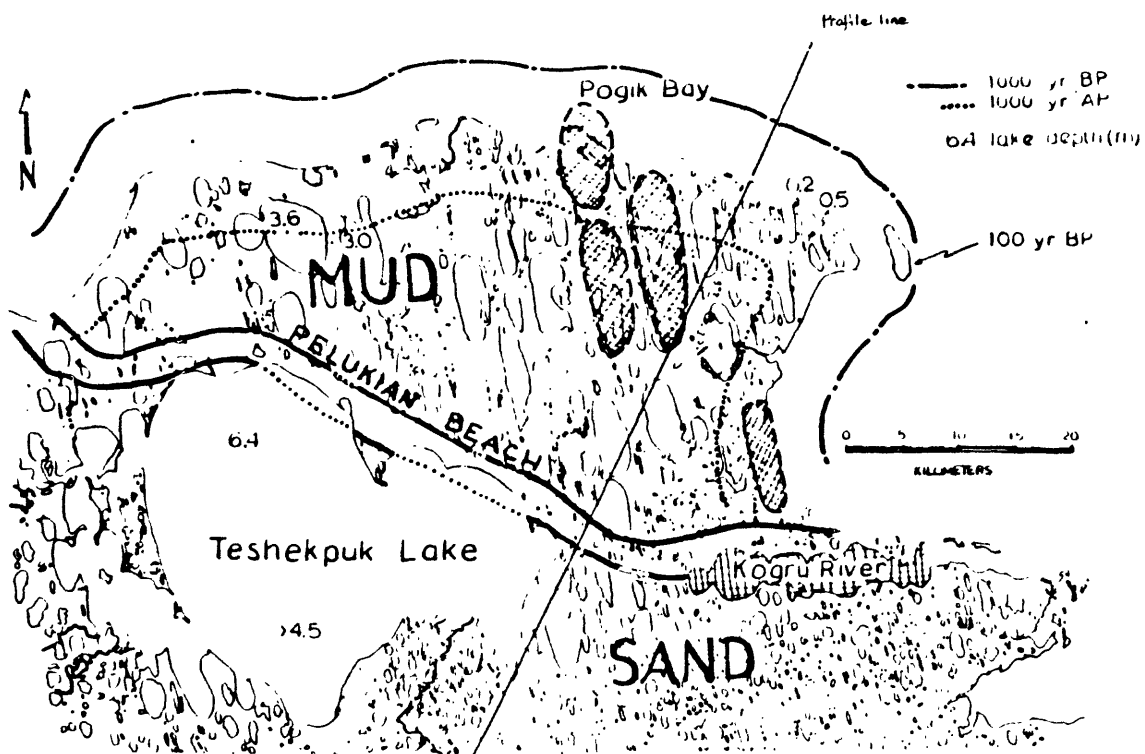


Figure 26. Map of Cape Halkett promontory, showing an old beachline/barrier chain separating two distinct types of surficial deposits; 1000 year hind- and forecast shorelines, lake depths, location of an early 19th century island called Cape Halkett and; the largest shallow lakes which may be candidates for thermal collapse, breaching, and resulting lagoon formation (Wiseman, et al., 1973) are shaded to show their distinction from present lagoons.

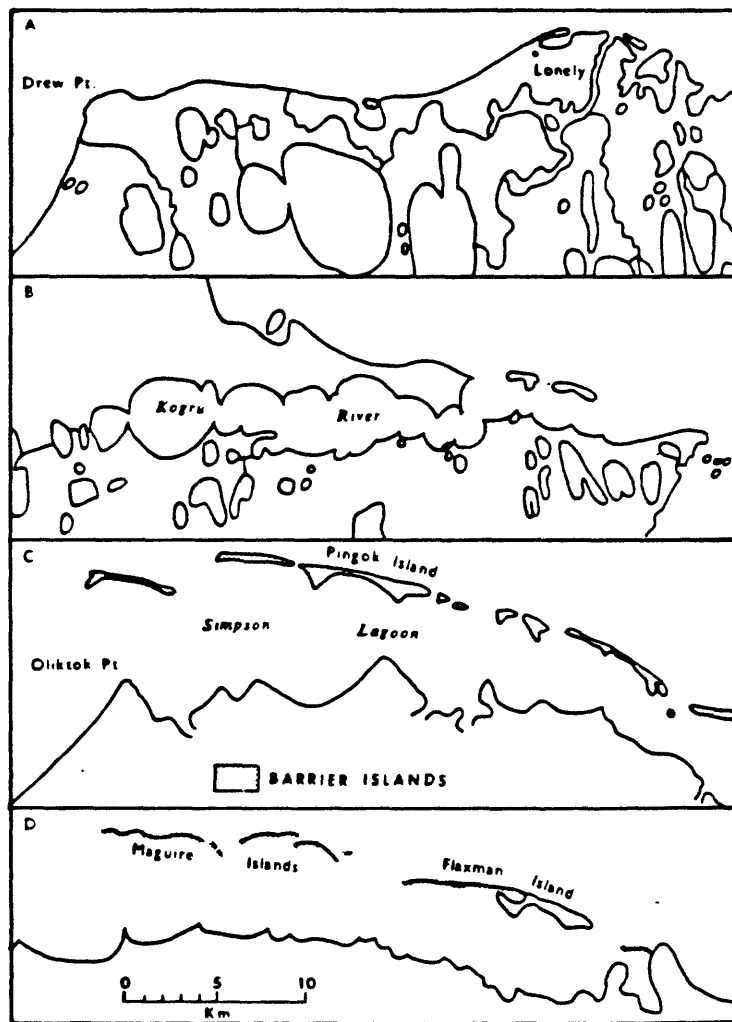


Figure 27. Sequence of lagoon formation and barrier island isolation by thaw-lake coalescence. A) initial tapping, draining, and coalescing of lakes, B) continued coalescing of lakes and thermal erosion of shoreline, C) continued thermal erosion and isolation of offshore tundra remnants, D) erosion of tundra remnants and reworking of sand and gravel into offshore barriers (from Wiseman, et.al., 1973).

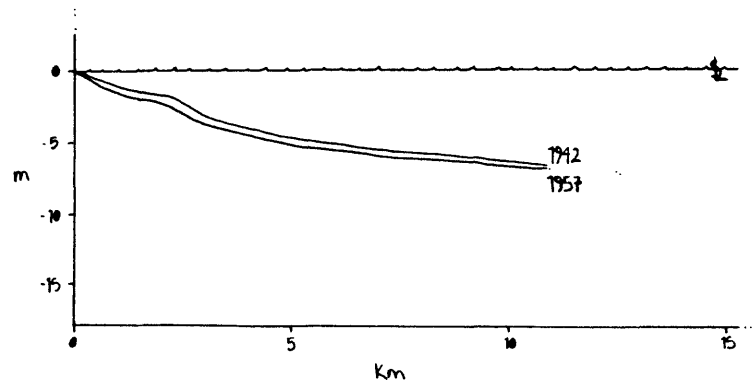


Figure 28. Comparison of hydrographic surveys repeated after 15 yrs in the East Siberian Sea (after Klyuyev 1965).

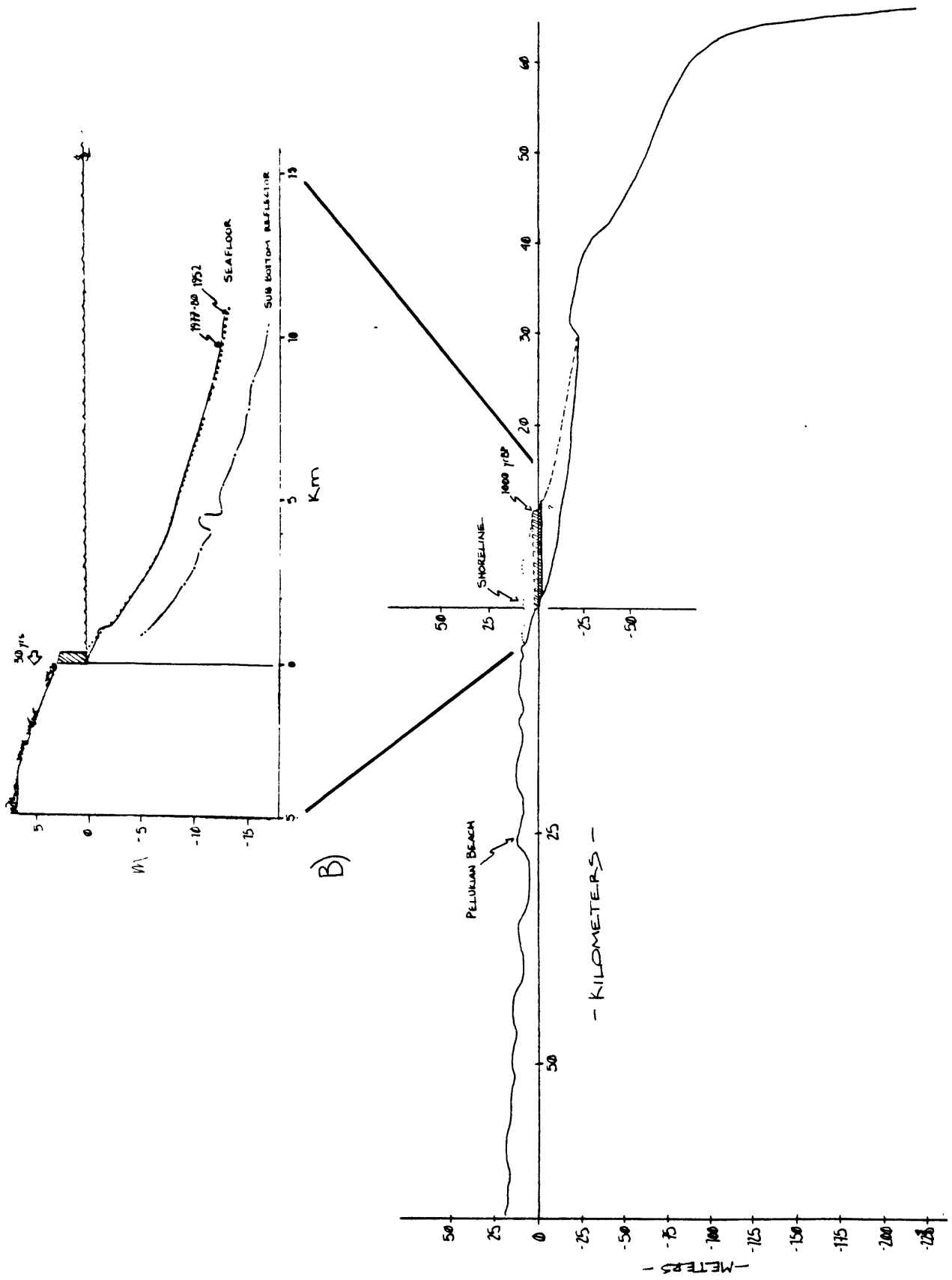


Figure 29 Coastal plain/shelf profile along line indicated on figure 26
 A) present profile and 1000 yr hindcast with accounted and unaccounted volumes indicated, B) detailed coastal zone profile showing a 30 year comparison of bluff and seafloor, and a shallow seismic reflector.

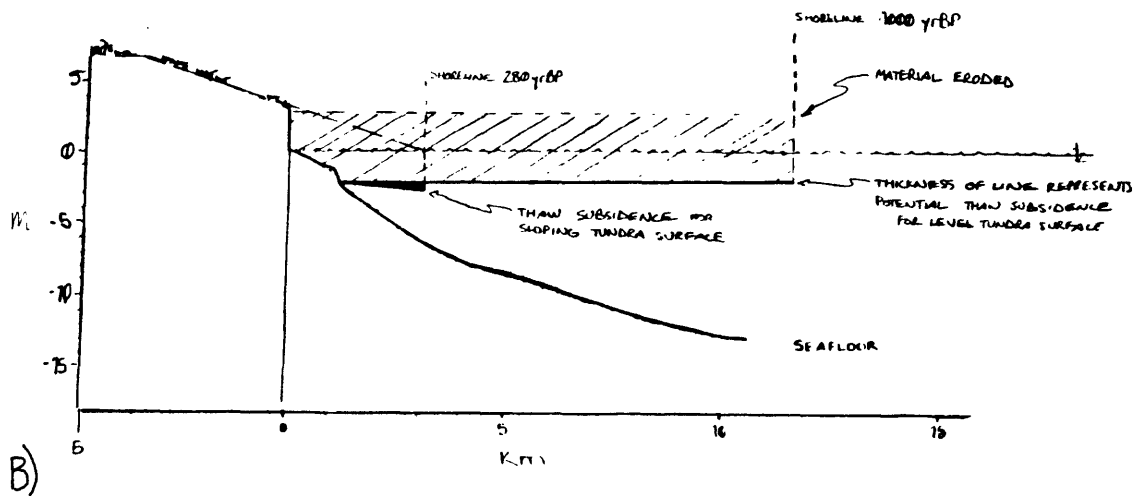
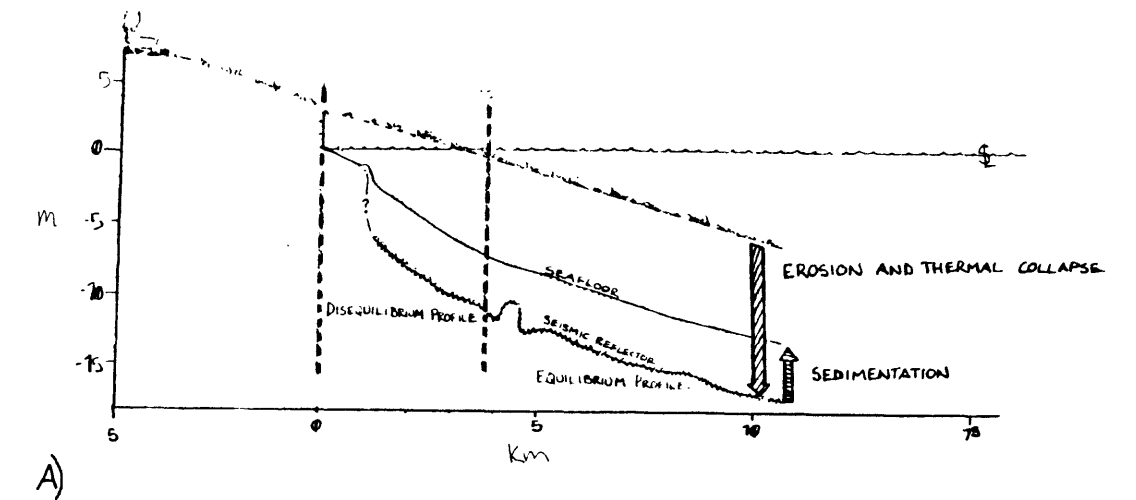


Figure 30. Same profile as figure 29B with hypothetical tundra surfaces, A) possible origin of the seismic reflector as the old land surface after erosion, thaw subsidence and Holocene sedimentation, and B) potential thaw settlement below the -2m truncation surface for both level and sloping tundra surfaces assuming deep thaw.

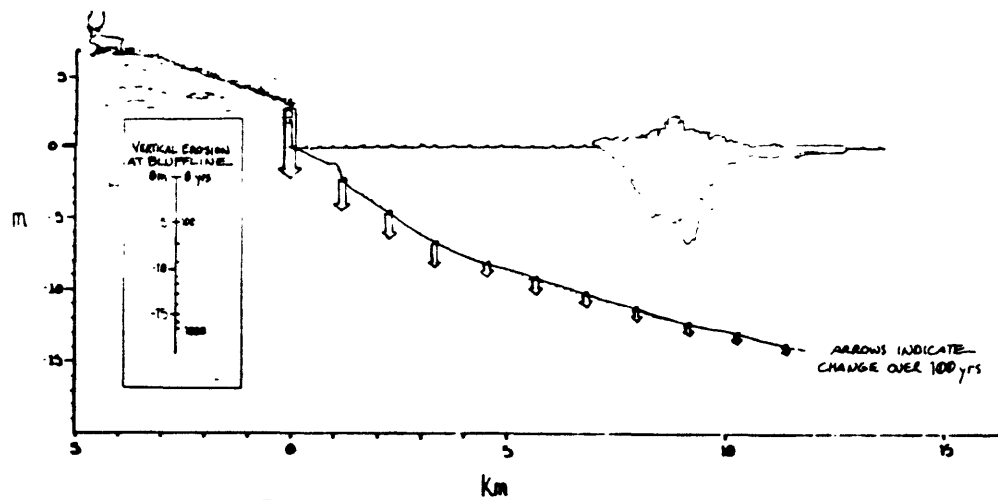


Figure 31. Present land and seafloor surface with arrows indicating vertical erosion predicted for the next hundred years at 1 km intervals along the profile; inset shows thousand year vertical erosion predicted for a point at the present shore.

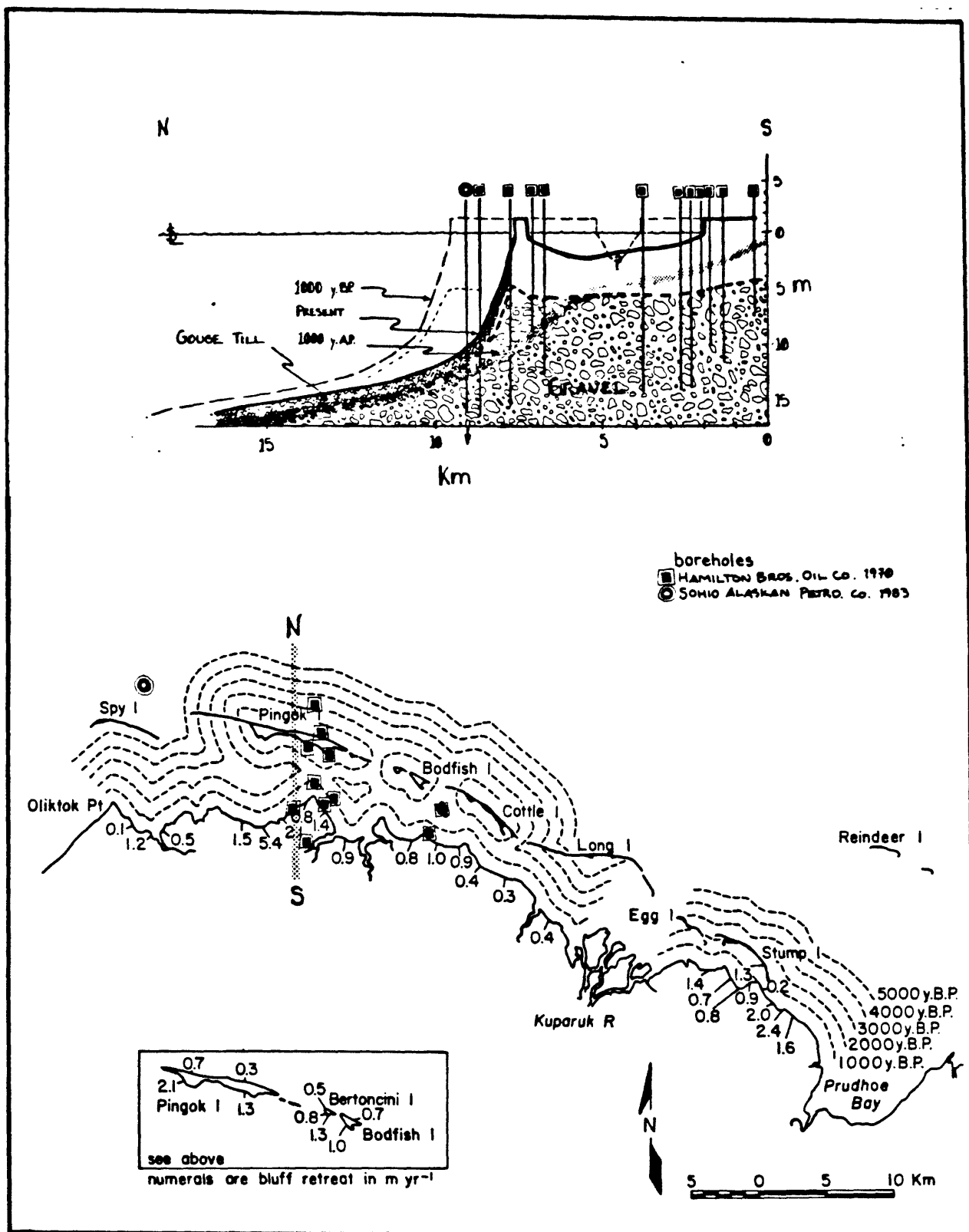


Figure 32. Simpson Lagoon paleoshorelines (after Naidu et al. 1984) and our interpretation of lagoon profile evolution. Depths to massive fluvial gravel generalised from soil borings.

APPENDIX (individual sector tabulations)

SECTOR # 1 Length: 19 km Average Retreat Rate: 8.3 m/yr

Segment No.	Onshore		Offshore		Totals	
	H	C	vi	v1	ϕ^*	tons
1	4.0	150	300000	246000	0.23	500
2	4.0	230	460000	380000	0.19	600
3	4.0	240	480000	394000	0.14	800
4	4.0	230	460000	380000	0.14	800
5	4.0	230	460000	380000	0.13	850
6	4.0	220	440000	360000	0.13	850
7	4.0	210	420000	344000	0.14	800
8	4.0	220	440000	360000	0.15	750
9	4.0	300	600000	492000	0.16	700
10	4.0	350	700000	574000	0.19	600
11	4.0	380	760000	623000	0.29	400
12	4.0	300	600000	492000	0.25	450
13	4.0	280	560000	459000	0.29	400
14	4.0	230	460000	377000	0.25	450
15	4.0	300	600000	492000	0.25	450
16	4.0	350	700000	574000	0.25	450
17	4.0	400	800000	656000	0.23	500
18	4.0	480	960000	787000	0.25	450
19	4.0	450	900000	738000	0.33	350
20	4.0	350	700000	574000	0.36	320
21	3.5	360	630000	498000	0.33	350
22	3.0	330	495000	376000	0.29	400
23	3.0	300	450000	342000	0.25	450
24	2.0	280	280000	196000	0.22	510
25	2.0	280	280000	196000	0.19	600
26	2.0	200	200000	140000	0.18	650
27	2.0	210	210000	147000	0.18	650
28	2.0	200	200000	140000	0.16	700
29	2.0	160	160000	112000	0.16	700
30	2.0	180	180000	124000	0.19	600
31	2.0	270	270000	189000	0.25	450
32	2.0	270	270000	189000	0.29	400
33	2.0	190	190000	133000	0.23	500
34	2.0	170	170000	119000	0.19	600
35	2.0	140	140000	98000	0.20	580
36	2.0	120	120000	84000	0.19	600
37	2.0	50	50000	35000	0.19	600
38	2.0	0	0	0	0.20	580
TOTALS ($\times 10^3$) :			16095	12800		6654
						19454
						36767

SECTOR # 2 Length: 12.5 km Average Retreat Rate: 1.3 m/yr

Segment No.	Onshore				Offshore				Totals	
	H	C	vi	v1	θ°	w	t	v2	volume	tons
1	1.5	0	0	0	0.23	500	0	0	0	0
2	1.5	20	15000	10000	0.29	400	0.10	19000	29000	55000
3	1.5	50	38000	25000	0.38	300	0.33	46000	71000	134000
4	1.5	100	75000	49000	0.46	250	0.80	80000	129000	244000
5	1.5	110	82000	53000	0.57	200	1.10	80000	133000	251000
6	1.5	90	68000	44000	0.55	210	0.86	71000	115000	217000
7	1.5	30	22000	14000	0.55	210	0.29	28000	42000	79000
8	1.5	30	22000	14000	0.67	170	0.35	27000	41000	77000
9	3.0	0	0	0	0.57	200	0	0	0	0
10	1.5	20	15000	10000	0.55	210	0.19	19000	29000	55000
11	0.4	60	12000	8000	0.88	130	0.92	46000	54000	102000
12	0.4	100	0	0	2.29	50	4.00	25000	25000	47000
13	0.4	80	0	0	1.64	70	2.29	24000	24000	45000
14	0.4	100	20000	13000	3.81	30	6.65	15000	28000	53000
15	1.5	60	45000	29000	3.81	30	3.99	15000	44000	83000
16	1.5	0	0	0	0.95	120	0	0	0	0
17	0.4	20	4000	3000	1.15	100	0.40	18000	21000	40000
18	0.4	120	24000	16000	3.81	30	7.98	15000	31000	59000
C 19	0.4	0	0	0	1.60	270	7.54	270000	270000	510000
C 20	0.4	0	0	0	1.60	270	7.54	270000	270000	510000
C 21	0.4	0	0	0	1.60	270	7.54	270000	270000	510000
C 22	0.4	0	0	0	1.60	270	7.54	270000	270000	510000
C 23	0.4	0	0	0	1.60	270	7.54	270000	270000	510000
24	1.5	20	15000	10000	0.36	150	0.13	19000	29000	55000
D 25	0.4	+20	0	0	0.36	320	0.06	+21000	+21000	+40000
TOTALS ($\times 10^3$) :			457	298				1876	2174	4106

SECTOR # 3 Length: 6 km Average Retreat Rate: 7.8 m/yr

Segment No.			Onshore		θ°	Offshore			Totals	
	H	C	v _i	v ₁		w	t		v ₂	volume tons
1	3.0	100	150000	114000	0.11	1000	0.20		95000	209000 395000
2	1.5	300	270000	176000	0.11	1000	0.60		255000	431000 815000
3	1.5	450	422000	274000	0.09	1200	0.75		366000	640000 1210000
4	1.5	280	240000	156000	0.09	1300	0.43		250000	406000 767000
5	1.5	40	30000	20000	0.07	1500	0.05		395000	415000 784000
6	1.5	100	76000	49000	0.05	2200	0.09		98000	147000 278000
7	1.5	220	166000	108000	0.05	2200	0.02		209000	317000 599000
8	1.5	270	167000	109000	0.04	2400	0.18		200000	309000 584000
9	1.5	300	245000	159000	0.05	2200	0.27		280000	439000 830000
10	1.5	190	152000	99000	0.06	2000	0.19		181000	280000 529000
11	1.5	310	245000	159000	0.05	2200	0.28		288000	447000 845000
12	1.5	200	160000	104000	0.06	2000	0.20		190000	294000 556000
TOTALS (x10 ³) :			2323	1527					2807	4334 8192

SECTOR # 4 Length: 11 km Average Retreat Rate: Pogik Bay ~ 0.4 m/yr, barrier ~ 7.3 m/yr

Segment No.	Onshore				Offshore		Totals			
	H	C	v_i	v_1	ϕ^o	w	t	v_2	volume	tons
D 1	1.5	+70	+52000	+52000	0		0	0	+52000	+98000
D 2	1.5	+100	+75000	+75000	0		0	0	+75000	+142000
D 3	1.5	+80	+60000	+60000	0		0	0	+60000	+113000
D 4	1.5	+120	+90000	+90000	0		0	0	+90000	+170000
5	1.5	0	0	0	0		0	0	0	0
D 6	2.0	+60	+60000	+60000	0		0	0	+60000	+113000
7	2.0	0	0	0	0		0	0	0	0
8	2.0	0	0	0	0		0	0	0	0
9	2.0	20	20000	14000	0		0	0	14000	26000
10	1.5	70	52000	34000	0		0	0	34000	64000
11	1.5	100	75000	49000	0		0	0	49000	93000
12	1.5	130	98000	64000	0		0	0	64000	121000
13	1.5	120	90000	59000	0		0	0	59000	112000
14	1.5	120	90000	59000	0		0	0	59000	112000
15	1.5	130	98000	64000	0		0	0	64000	121000
16	1.5	170	127000	83000	0		0	0	83000	157000
17	1.5	200	150000	98000	0		0	0	98000	185000
18	1.5	200	150000	98000	0		0	0	98000	185000
D 19	0.2	+100	+10000	+10000	0.06	2000	0.10	+95000	+105000	+198000
D 20	0.2	+300	+30000	+30000	0.05	2200	0.26	+298000	+328000	+620000
21	0.2	0	0	0	0.05	2200	0	0	0	0
D 22	0.2	+200	+20000	+20000	0.06	2000	0.21	+201000	+221000	+418000
C Offshore input for migrating barrier at bay mouth :								1972000	1972000	3727000
TOTALS ($\times 10^3$) :			553	225				1378	1603	3030

SECTOR # 5 Length: 22.5 km Average Retreat Rate: 7.4 m/yr

Segment No.	Onshore		Offshore		Totals	
	H	C	vi	v1	volume	tons
D 1	0.2	+80	+8000	+8000	+86000	+163000
2	2.0	100	100000	70000	167000	316000
3	2.0	70	70000	49000	118000	223000
4	2.0	100	100000	70000	168000	318000
5	2.0	250	250000	175000	411000	777000
6	2.0	500	500000	350000	772000	1459000
7	2.0	480	480000	366000	769000	1453000
8	3.0	300	450000	342000	612000	1157000
9	2.0	160	160000	122000	273000	516000
10	2.0	120	120000	84000	199000	376000
11	2.0	110	110000	77000	183000	346000
12	2.0	140	140000	98000	230000	435000
13	3.0	60	90000	68000	127000	240000
14	2.0	110	110000	77000	181000	342000
15	3.0	100	150000	114000	209000	395000
16	2.0	180	180000	126000	283000	535000
17	4.0	210	420000	344000	532000	1006000
18	2.0	340	340000	238000	525000	992000
19	2.0	410	410000	287000	613000	1159000
20	2.0	400	400000	280000	600000	1134000
21	2.0	280	280000	196000	436000	824000
22	4.0	300	600000	492000	742000	1402000
23	2.0	260	260000	182000	404000	764000
24	2.0	250	250000	175000	390000	737000
25	3.0	130	195000	148000	270000	510000
26	3.0	110	165000	125000	229000	433000
27	2.0	120	120000	84000	197000	372000
28	2.0	250	250000	175000	394000	745000
29	2.0	300	300000	210000	463000	875000
30	3.0	300	450000	342000	596000	1126000
31	3.0	300	450000	342000	597000	1128000
32	2.0	260	260000	182000	407000	769000
33	2.0	310	310000	217000	474000	896000
34	2.0	400	400000	280000	569000	1075000
35	3.0	400	600000	456000	723000	1367000
36	2.0	300	300000	210000	435000	822000
37	2.0	250	250000	175000	360000	680000
38	2.0	120	120000	84000	190000	359000
39	3.0	80	120000	91000	166000	314000
40	3.0	70	105000	80000	147000	278000
41	3.0	100	150000	114000	209000	395000
42	1.0	100	50000	30000	126000	238000
43	1.0	200	100000	60000	247000	467000
44	1.0	370	185000	111000	435000	822000
45	1.0	400	200000	120000	480000	907000
TOTALS (x10 ³) :			11042	8010	16572	31321

SECTOR # 6 Length: 24 km Average Retreat Rate: 2.9 m/yr

Segment No.	Onshore		Offshore		Totals					
	H	C	vi	v1	⊖°	w	t	v2	volume	tons
1	2.0	100	100000	70000	0.14	800	0.25	94000	164000	310000
2	3.5	130	227000	179000	0.14	820	0.32	120000	299000	565000
3	3.5	100	175000	138000	0.11	1000	0.20	95000	233000	440000
4	3.5	100	175000	138000	0.11	1000	0.20	95000	233000	440000
5	3.5	90	158000	124000	0.11	1000	0.18	86000	210000	397000
6	3.5	100	175000	138000	0.13	900	0.22	94000	232000	438000
7	3.5	110	192000	151000	0.16	700	0.31	101000	252000	476000
8	3.5	120	210000	166000	0.16	700	0.34	110000	276000	522000
9	2.0	110	110000	77000	0.14	800	0.27	102000	179000	338000
10	2.0	130	130000	91000	0.13	850	0.31	120000	211000	399000
11	2.0	140	140000	98000	0.13	850	0.33	1128000	1226000	2317000
12	3.0	110	165000	125000	0.13	900	0.24	103000	228000	431000
13	3.0	100	150000	114000	0.12	940	0.21	95000	209000	395000
14	3.5	80	140000	111000	0.12	920	0.17	77000	188000	355000
15	3.5	50	88000	70000	0.13	910	0.11	49000	119000	225000
16	3.5	0	0	0	0.10	1100	0	0	0	0
17	3.5	20	35000	28000	0.10	1200	0.03	20000	48000	91000
18	3.5	40	70000	55000	0.09	1250	0.06	39000	94000	178000
19	3.5	30	52000	41000	0.07	1700	0.04	89000	130000	246000
20	3.5	100	175000	138000	0.07	1700	0.12	97000	235000	444000
21	2.0	100	100000	70000	0.08	1400	0.14	96000	166000	314000
22	2.0	100	100000	70000	0.07	1600	0.12	97000	167000	316000
23	1.0	150	75000	45000	0.07	1700	0.18	143000	188000	355000
24	1.0	110	55000	33000	0.09	1250	0.18	105000	138000	261000
25	2.0	100	100000	70000	0.08	1350	0.15	96000	166000	314000
26	3.0	110	165000	125000	0.09	1250	0.18	105000	230000	435000
27	3.0	110	165000	125000	0.13	900	0.24	120000	245000	463000
28	3.0	80	120000	91000	0.08	1500	0.11	78000	169000	319000
29	3.0	60	90000	68000	0.08	1500	0.08	59000	127000	240000
30	3.0	100	150000	114000	0.08	1500	0.13	97000	211000	399000
31	3.0	150	225000	171000	0.08	1500	0.20	143000	314000	593000
32	3.0	130	195000	148000	0.08	1500	0.17	124000	272000	514000
33	3.0	110	165000	125000	0.08	1500	0.15	106000	231000	437000
34	3.0	110	165000	125000	0.09	1300	0.17	105000	230000	435000
35	3.0	100	150000	114000	0.07	1600	0.12	97000	211000	399000
36	3.0	100	150000	114000	0.06	2000	0.10	98000	212000	401000
37	3.0	100	150000	114000	0.04	3000	0.07	98000	212000	401000
38	3.0	100	150000	114000	0.04	3000	0.07	98000	212000	401000
39	3.0	120	185000	140000	0.03	3300	0.07	118000	258000	488000
40	3.0	110	165000	125000	0.03	3600	0.06	108000	233000	440000
41	3.0	80	120000	91000	0.03	3500	0.05	79000	170000	321000
42	3.0	40	60000	46000	0.03	3400	0.02	40000	86000	162000
43	3.0	20	30000	23000	0.03	3400	0.01	20000	43000	81000
44	3.0	20	30000	23000	0.03	3400	0.01	20000	43000	81000
45	3.0	20	30000	23000	0.03	3400	0.01	20000	43000	81000
46	3.0	20	30000	23000	0.03	3400	0.01	20000	43000	81000
47	3.0	40	60000	46000	0.03	3400	0.02	40000	86000	163000
48	4.0	70	140000	115000	0.03	3400	0.04	69000	184000	348000
TOTALS (x10 ³):			5987	4543				5113	9656	18250

SECTOR # 7 Length: 24.5 km Average Retreat Rate: 1.4 m/yr

Segment No.	Onshore		Offshore		Totals					
	H	C	vi	v1	⊖°	w	t	v2	volume	tons
1	3.0	90	135000	103000	0.03	4000	0.05	89000	192000	363000
2	3.0	110	165000	125000	0.03	4000	0.06	108000	233000	440000
3	3.0	100	150000	114000	0.04	3000	0.07	98000	212000	401000
4	3.0	60	90000	68000	0.04	2800	0.04	59000	127000	240000
5	3.0	0	0	0	0.04	2600	0	0	0	0
6	3.0	100	150000	114000	0.05	2500	0.08	98000	212000	401000
7	3.0	90	135000	103000	0.06	2000	0.09	88000	191000	361000
8	3.0	180	270000	205000	0.08	1400	0.26	168000	373000	705000
9	3.0	0	0	0	0.10	1200	0	0	0	0
10	3.0	140	210000	160000	0.15	750	0.37	127000	287000	543000
11	3.0	130	195000	148000	0.79	600	0.43	116000	264000	499000
12	3.0	100	150000	114000	0.23	500	0.39	90000	204000	386000
13	4.0	20	40000	33000	0.23	500	0.08	20000	53000	100000
14	4.0	20	40000	33000	0.21	550	0.07	20000	53000	100000
15	4.0	0	0	0	0.23	500	0	0	0	0
16	4.0	0	0	0	0.79	600	0	0	0	0
17	3.0	20	30000	23000	0.13	850	0.05	20000	43000	81000
18	3.0	20	30000	23000	0.12	950	0.04	20000	43000	81000
19	3.0	50	75000	57000	0.11	1050	0.10	49000	106000	200000
20	3.0	50	75000	57000	0.10	1150	0.10	49000	106000	200000
21	3.0	30	90000	68000	0.10	1150	0.10	49000	117000	221000
22	5.0	0	0	0	0.10	1100	0	0	0	0
23	5.0	0	0	0	0.10	1100	0	0	0	0
24	5.0	30	75000	57000	0.10	1150	0.05	30000	87000	164000
25	3.0	60	90000	68000	0.10	1200	0.10	59000	127000	240000
26	3.0	60	90000	68000	0.09	1250	0.10	59000	127000	240000
27	5.0	70	175000	148000	0.09	1300	0.11	68000	216000	408000
28	5.0	50	125000	108000	0.08	1350	0.15	96000	204000	386000
29	1.0	100	50000	30000	0.08	1350	0.15	96000	126000	238000
30	4.0	0	0	0	0.05	2500	0	0	0	0
31	4.0	0	0	0	0.05	2500	0	0	0	0
32	4.0	0	0	0	0.05	2500	0	0	0	0
33	4.0	0	0	0	0.05	2500	0	0	0	0
34	4.0	0	0	0	0.05	2500	0	0	0	0
35	4.0	0	0	0	0.05	2500	0	0	0	0
36	4.0	0	0	0	0.05	2500	0	0	0	0
37	4.0	0	0	0	0.05	2500	0	0	0	0
38	4.0	0	0	0	0.05	2500	0	0	0	0
39	4.0	0	0	0	0.05	2500	0	0	0	0
40	4.0	0	0	0	0.05	2500	0	0	0	0
41	4.0	0	0	0	0.05	2500	0	0	0	0
42	2.0	0	0	0	0.05	2500	0	0	0	0
43	2.0	0	0	0	0.05	2500	0	0	0	0
44	2.0	30	30000	21000	0.04	3200	0.02	30000	51000	96000
45	2.0	70	70000	49000	0.04	2600	0.05	69000	118000	223000
46	2.0	60	60000	42000	0.05	2300	0.05	59000	101000	191000
47	2.0	100	100000	70000	0.06	1900	0.10	97000	167000	316000
48	1.0	100	50000	30000	0.07	1600	0.12	97000	127000	240000
49	1.0	20	50000	30000	0.08	1450	0.03	20000	50000	95000

Input not calculated for Eskimo Islands; no significant net change.

TOTALS ($\times 10^3$) : 2295 2269 2048 4317 8159

SECTOR # 8 Length: 8.5 km Average Retreat Rate: 1.7 m/yr

Segment No.	Onshore				Offshore				Totals	
	H	C	vi	v1	ϕ	w	t	v2	volume	tons
1	2.0	70	70000	49000	0.05	2400	0.06	69000	118000	223000
2	2.0	70	70000	49000	0.04	3000	0.05	69000	118000	223000
3	2.0	50	50000	35000	0.03	3500	0.03	49000	84000	159000
4	2.0	0	0	0	0.03	3300	0	0	0	0
5	2.0	0	0	0	0.03	3500	0	0	0	0
6	2.0	0	0	0	0.03	3600	0	0	0	0
7	2.0	0	0	0	0.03	3800	0	0	0	0
8	2.0	20	20000	14000	0.03	4000	0.01	20000	34000	64000
9	2.0	50	50000	35000	0.03	4000	0.03	50000	85000	161000
12	2.0	0	0	0	0.03	4000	0	0	0	0
11	2.0	0	0	0	0	0	0	0	0	0
12	2.0	0	0	0	0	0	0	0	0	0
13	2.0	0	0	0	0	0	0	0	0	0
14	2.0	0	0	0	0	0	0	0	0	0
15	2.0	0	0	0	0	0	0	0	0	0
16	2.0	0	0	0	0	0	0	0	0	0
17	2.0	30	30000	21000	0.05	2500	0.20	30000	51000	96000
18	2.0	20	20000	14000	0.05	2500	0.20	20000	34000	64000
19	2.0	0	0	0	0.05	2300	0	0	0	0

Total of Offshore spits, bars, flats :

126000 23814000

TOTALS ($\times 10^3$) :

562 469

433

902

1705

SECTOR # 9 Length: 23 km Average Retreat Rate: 0.7 m/yr

Segment No.	Onshore				Offshore				Totals	
	H	C	vi	v1	⊖°	w	t	v2	volume	tons
1	3.0	0	0	0	0.08	1500	0	0	0	0
2	4.0	0	0	0	0.08	1500	0	0	0	0
3	3.0	0	0	0	0.08	1500	0	0	0	0
4	3.0	0	0	0	0.08	1500	0	0	0	0
5	4.0	0	0	0	0.10	1200	0	0	0	0
6	2.0	0	0	0	0.09	1300	0	0	0	0
7	3.0	0	0	0	0.10	1200	0	0	0	0
8	2.0	0	0	0	0.09	1300	0	0	0	0
9	5.0	0	0	0	0.09	1300	0	0	0	0
10	3.0	0	0	0	0.07	1600	0	0	0	0
11	2.0	20	20000	14000	0.07	1600	0.03	20000	34000	64000
12	3.0	0	0	0	0.07	1600	0	0	0	0
13	3.0	20	30000	23000	0.07	1600	0.03	20000	43000	81000
14	4.0	20	40000	33000	0.07	1700	0.02	20000	53000	100000
15	2.0	20	20000	14000	0.07	1700	0.02	20000	34000	64000
16	2.0	40	40000	28000	0.08	1500	0.05	39000	67000	127000
17	4.0	40	80000	66000	0.08	1500	0.05	39000	105000	198000
18	2.0	100	100000	70000	0.08	1500	0.13	97000	167000	316000
19	2.0	20	20000	14000	0.08	1400	0.29	20000	34000	64000
D 20	0.2	+130	+13000	+13000	0.08	1400	0.18	+129000	+142000	+268000
21	2.0	100	100000	70000	0.10	1200	0.17	96000	166000	314000
22	2.0	80	80000	56000	0.08	1500	0.11	78000	134000	253000
23	2.0	60	60000	42000	0.06	2000	0.06	59000	101000	191000
24	2.0	70	70000	49000	0.06	2000	0.07	69000	118000	223000
25	2.0	70	70000	49000	0.07	1700	0.08	69000	118000	223000
26	3.0	60	90000	68000	0.08	1400	0.09	59000	127000	240000
27	3.0	0	0	0	0.08	1500	0	0	0	0
28	3.0	20	20000	15000	0.06	1800	0.02	20000	35000	66000
29	4.0	50	100000	82000	0.06	1800	0.06	49000	131000	248000
30	3.0	110	165000	125000	0.06	1800	0.12	107000	232000	438000
31	3.0	30	45000	34000	0.06	1900	0.03	30000	64000	121000
32	3.0	40	60000	46000	0.05	2300	0.03	40000	86000	163000
33	2.0	40	40000	28000	0.05	2300	0.03	40000	68000	129000
34	2.0	20	20000	14000	0.05	2300	0.02	20000	34000	64000
35	3.0	30	45000	34000	0.05	2300	0.03	30000	64000	121000
36	4.0	20	40000	33000	0.05	2300	0.02	20000	53000	100000
37	3.0	0	0	0	0.05	2300	0	0	0	0
38	3.0	20	30000	23000	0.05	2300	0.02	20000	43000	81000
39	4.0	20	40000	33000	0.05	2300	0.02	20000	53000	100000
40	4.0	20	40000	33000	0.05	2300	0.02	20000	53000	100000
41	3.0	0	0	0	0.05	2300	0	0	0	0
42	3.0	0	0	0	0.05	2300	0	0	0	0
43	3.0	0	0	0	0.05	2300	0	0	0	0
44	4.0	0	0	0	0.05	2300	0	0	0	0
45	2.0	0	0	0	0.06	2300	0	0	0	0
46	2.0	0	0	0	0.06	2300	0	0	0	0
TOTALS	(x10 ³) :		1452	1083				992	2075	3922

SECTOR # 10 Length: 15.5 km Average Retreat Rate: 2.5 m/yr

Segment No.	Onshore		Offshore		Totals	
	H	C	vi	v1	volume	tons
1	1.5	50	38000	25000	75000	142000
2	1.5	30	22000	14000	44000	83000
3	1.5	20	15000	10000	30000	57000
4	1.5	20	15000	10000	30000	57000
5	1.5	0	0	0	0	0
6	3.0	0	0	0	0	0
7	1.5	20	15000	10000	30000	57000
8	1.5	60	45000	29000	89000	168000
9	1.5	100	75000	49000	148000	280000
10	1.5	130	98000	64000	193000	365000
11	1.5	90	68000	44000	134000	253000
12	1.5	100	75000	49000	148000	280000
13	1.5	90	68000	44000	134000	253000
14	1.5	80	60000	39000	119000	225000
15	1.5	90	68000	44000	134000	253000
16	1.5	120	90000	59000	178000	336000
17	1.0	20	10000	6000	26000	49000
18	1.0	40	20000	12000	52000	98000
19	1.0	60	30000	18000	78000	147000
20	1.0	100	50000	30000	129000	244000
21	1.0	140	70000	42000	181000	342000
22	1.0	200	100000	60000	258000	488000
23	1.0	100	50000	30000	129000	244000
24	1.0	90	45000	27000	117000	221000
25	1.0	90	45000	27000	117000	221000
26	1.0	80	40000	24000	104000	197000
27	1.0	90	45000	27000	117000	221000
28	1.0	60	30000	18000	78000	147000
29	1.5	70	53000	34000	104000	196000
30	1.5	100	75000	49000	149000	282000
31	1.5	50	38000	25000	75000	142000
TOTALS (x10 ³) :			1453	919	2281	6048

SECTOR # 11 Length: 48 km Average Retreat Rate: +.4 m/yr

Segment No.	Onshore				Offshore				Totals	
	H	C	vi	v1	θ°	w	t	v2	volume	tons
1	0.5	40	10000	6000	0.01	14000	0.006	40000	46000	87000
2	0.5	20	5000	3000	0.01	13600	0.003	20000	23000	43000
3	0.5	40	10000	6000	0	0	0	0	6000	11000
4	0.5	30	7000	4000	0	0	0	0	4000	8000
5	0.5	20	5000	3000	0	0	0	0	3000	6000
6	0.5	50	12000	7000	0	0	0	0	7000	13000
7	0.5	50	12000	7000	0	0	0	0	7000	13000
8	0.5	20	5000	3000	0	0	0	0	3000	6000
D 9	0.2	+60	+6000	+6000	0	0	0	0	+6000	+11000
10	0.5	0	0	0	0.1	3500	0	0	0	0
11	0.5	100	25000	14000	0.01	12400	0.10	70000	84000	159000
12	0.5	80	20000	11000	0	0	0	0	11000	21000
13	0.5	20	5000	3000	0	0	0	0	3000	6000
14	0.5	0	0	0	0.01	11000	0	0	0	0
15	0.5	30	7000	4000	0.01	10450	0.01	50000	54000	102000
16	0.5	80	20000	11000	0	0	0	0	11000	21000
17	0.4	100	20000	20000	0.01	9700	0.02	99000	119000	225000
18	0.4	70	14000	14000	0.01	8900	0.02	70000	84000	159000
19	0.4	90	18000	18000	0.01	8600	0.02	90000	108000	204000
20	0.4	110	22000	22000	0.01	8000	0.03	110000	132000	249000
21	0.4	230	46000	46000	0.02	7400	0.06	226000	272000	514000
22	0.4	160	32000	32000	0.02	7200	0.04	158000	190000	359000
D 23	0.2	+110	+11000	+11000	0.02	7200	0.03	+109000	+120000	+227000
24	0.4	140	28000	28000	0.02	7200	0.04	139000	167000	316000
D 25	0.2	+220	+22000	+22000	0.02	7100	0.06	+217000	+239000	+452000
26	0.5	0	0	0	0.01	8200	0	0	0	0
D 27	0.2	+150	+15000	+15000	0.01	8700	0.03	+149000	+164000	+310000
D 28	0.2	+110	+11000	+11000	0.01	8600	0.02	+109000	+120000	+227000
D 29	0.2	+20	+2000	+2000	0.01	8500	0.004	+20000	+22000	+42000
30	0.5	200	50000	29000	0.01	8100	0.04	197000	226000	427000
31	0.5	300	75000	43000	0.01	7900	0.07	294000	337000	637000
32	0.5	0	0	0	0.01	8300	0	0	0	0
33	0.5	210	52000	30000	0.01	9480	0.04	208000	238000	450000
34	0.5	200	50000	29000	0.01	10000	0.04	198000	227000	429000
35	1.0	0	0	0	0.01	10000	0	0	0	0
36	1.0	80	40000	24000	0.01	9500	0.02	80000	104000	197000
37	1.0	20	20000	12000	0.01	9650	0.004	20000	32000	60000
D 38	0.2	+100	+10000	+10000	0.01	10100	0.02	+99000	+109000	+206000
D 39	1.0	70	70000	42000	0.01	10300	0.01	70000	112000	212000
40	1.0	100	100000	60000	0.01	9800	0.02	99000	159000	301000
41	1.0	110	110000	66000	0.01	9300	0.02	109000	175000	331000
D 42	0.2	+20	+2000	+2000	0.01	9200	0.004	+20000	+22000	+42000
43	1.0	40	40000	24000	0.01	9100	0.01	40000	64000	121000
44	1.0	30	30000	18000	0.01	9000	0.006	30000	48000	91000
45	1.0	40	40000	24000	0.01	8900	0.01	40000	64000	121000
46	1.0	0	0	0	0.01	9300	0	0	0	0
47	1.0	100	100000	60000	0.01	9750	0.02	10000	70000	132000
48	1.0	200	200000	120000	0.01	10000	0.04	198000	318000	601000
49	1.0	100	100000	60000	0.01	10100	0.02	99000	159000	301000
50	0.5	110	28000	16000	0.01	10150	0.02	11000	27000	51000
51	0.5	120	30000	17000	0.01	10200	0.02	119000	136000	257000
52	0.5	120	30000	17000	0.01	10300	0.02	119000	136000	257000
53	0.5	100	25000	14000	0.01	10000	0.02	99000	113000	214000
54	0.5	120	30000	17000	0.01	9700	0.02	119000	136000	257000
D 55	0.2	+30	+3000	+3000	0.01	9400	0.006	+30000	+33000	+62000
D 56	0.2	+220	+22000	+22000	0.01	8800	0.05	+217000	+239000	+452000
57	0.2	90	9000	9000	0.01	8300	0.02	90000	99000	187000
58	0.2	320	32000	32000	0.01	7700	0.08	313000	345000	652000
59	0.2	280	28000	28000	0.02	7250	0.08	274000	302000	571000
60	0.2	160	16000	16000	0.02	7200	0.04	160000	176000	333000

(sector 11 continued)

61	0.2	200	20000	20000	0.02	7200	0.05	197000	217000	410000
62	0.2	0	0	0	0.02	7200	0	0	0	0
63	0.2	0	0	0	0.01	7700	0	0	0	0
64	0.2	0	0	0	0.01	7850	0	0	0	0
D 65	0.2	+300	+30000	+30000	0.01	7900	0.08	+290000	+320000	+605000
D 66	0.2	+410	+41000	+41000	0.01	7700	0.10	+399000	+440000	+832000
D 67	0.2	+400	+40000	+40000	0.01	7400	0.11	+389000	+429000	+811000
68	0.2	0	0	0	0.01	7600	0	0	0	0
69	0.2	0	0	0	0.01	7400	0	0	0	0
70	0.2	100	10000	10000	0.02	7100	0.02	99000	109000	206000
71	0.2	200	20000	20000	0.02	6950	0.05	197000	217000	410000
72	0.2	200	20000	20000	0.02	6900	0.06	197000	217000	410000
73	0.2	210	21000	20000	0.02	6700	0.06	207000	227000	429000
74	0.2	160	16000	16000	0.02	6250	0.05	158000	174000	329000
D 75	0.2	+60	+6000	+6000	0.02	5700	0.02	+60000	+66000	+125000
D 76	0.2	+500	+50000	+50000	0.02	5400	0.18	+477000	+527000	+996000
D 77	0.2	+600	+60000	+60000	0.02	5320	0.22	+566000	+626000	+1183000
D 78	0.2	+400	+40000	+40000	0.02	5400	0.15	+385000	+425000	+803000
D 79	0.2	+220	+22000	+22000	0.02	5500	0.08	+216000	+238000	+450000
D 80	0.2	+300	+30000	+30000	0.02	5300	0.11	+291000	+321000	+607000
D 81	0.2	+300	+30000	+30000	0.02	5100	0.12	+291000	+321000	+607000
D 82	0.2	+350	+35000	+35000	0.02	5000	0.14	+338000	+373000	+705000
D 83	0.2	+300	+30000	+30000	0.02	5400	0.11	+292000	+322000	+609000
D 84	0.2	+200	+20000	+20000	0.02	5100	0.08	+196000	+216000	+408000
85	0.2	0	0	0	0.02	6700	0	0	0	0
86	0.2	20	2000	2000	0.02	6550	0.006	20000	22000	42000
D 87	0.2	+200	+20000	+20000	0.01	8500	0.02	+80000	+100000	+189000
D 88	0.2	+100	+10000	+10000	0	0	0	0	+10000	+19000
89	0.2	100	10000	10000	0	0	0	0	10000	19000
90	0.2	120	12000	12000	0	0	0	0	12000	23000
91	0.2	80	8000	8000	0	0	0	0	8000	15000
92	0.2	60	6000	6000	0	0	0	0	6000	11000
93	0.2	100	10000	10000	0	0	0	0	10000	19000
94	0.2	90	9000	9000	0	0	0	0	9000	17000

D Total of Offshore spits, bars, flats :

+68000 +680000 +1285000

TOTALS (x10³) : 624 664

+777 +113 +214

SECTOR # 12 Length: 16.5 km Average Retreat Rate: 1.6 m/yr

Segment No.	Onshore				Offshore				Totals	
	H	C	v1	v1	θ^*	w	t	v2	volume	tons
1	1.0	40	20000	12000	0.02	6000	0.01	40000	52000	98000
2	1.0	40	20000	12000	0.02	6000	0.01	40000	52000	98000
3	1.0	20	10000	6000	0.02	5500	0.01	20000	26000	49000
4	1.0	60	30000	18000	0.02	5500	0.02	60000	78000	147000
5	1.0	30	15000	9000	0.02	4500	0.01	30000	39000	74000
6	1.0	20	10000	6000	0.02	4700	0.01	20000	26000	49000
7	1.0	20	10000	6000	0.02	4700	0.01	20000	26000	49000
8	1.0	80	41000	25000	0.03	3500	0.05	79000	104000	197000
9	1.0	80	42000	25000	0.01	1300	0.12	78000	103000	195000
10	1.0	70	37000	22000	0.11	1100	0.13	68000	90000	170000
11	1.5	100	90000	59000	0.15	750	0.29	102000	161000	304000
12	1.5	100	82000	53000	0.16	700	0.29	93000	146000	276000
13	1.5	100	83000	54000	0.19	600	0.33	92000	146000	276000
14	2.0	100	110000	77000	0.23	500	0.40	92000	169000	319000
15	2.0	110	111000	78000	0.23	500	0.44	98000	176000	333000
16	2.0	80	84000	57000	0.14	800	0.20	76000	133000	251000
17	2.0	80	80000	56000	0.10	1100	0.14	77000	133000	251000
18	2.5	40	50000	37000	0.17	650	0.12	39000	76000	144000
19	2.0	70	70000	49000	0.19	600	0.23	66000	115000	217000
20	2.0	30	30000	21000	0.19	600	0.10	29000	50000	95000
21	2.25	20	22000	16000	0.16	700	0.06	20000	36000	68000
22	2.25	20	22000	16000	0.19	600	0.07	20000	36000	68000
23	1.0	0	0	0	0.19	600	0	0	0	0
24	1.25	0	0	0	0.19	600	0	0	0	0
25	2.0	0	0	0	0.19	600	0	0	0	0
26	2.0	0	0	0	0.19	600	0	0	0	0
27	1.0	0	0	0	0.23	500	0	0	0	0
28	2.0	20	20000	14000	0.19	600	0.07	20000	34000	64000
29	2.0	20	20000	14000	0.19	600	0.02	20000	34000	64000
30	1.0	20	10000	6000	0.16	700	0.02	20000	26000	49000
31	1.0	20	10000	6000	0.16	700	0.02	20000	26000	49000
32	1.0	110	65000	39000	0.16	700	0.11	101000	140000	265000
33	1.0	100	50000	30000	0.19	600	0.33	92000	122000	231000
TOTALS ($\times 10^3$) :			1244	823				1532	2355	4450

SECTOR # 13 Length: 32 km Average Retreat Rate : 1.2 m/yr

Segment No.	Onshore		Offshore		Totals					
	H	C	vi	v1	ϕ°	w	t	v2	volume	tons
1	1.0	20	10000	6000	0.38	300	0.13	19000	25000	47000
2	2.0	20	20000	14000	0.16	700	0.06	20000	34000	64000
3	1.5	40	30000	20000	0.13	900	0.09	39000	59000	111000
4	1.5	50	38000	25000	0.11	1000	0.10	49000	74000	140000
5	1.5	0	0	0	0.07	1600	0	0	0	0
6	1.75	20	17000	11000	0.07	1700	0.02	20000	31000	59000
7	2.0	0	0	0	0.07	1700	0	0	0	0
D 8	0.2	+100	+10000	+10000	0.05	2300	0.09	+103000	+113000	+214000
D 9	0.2	+20	+2000	+2000	0.06	2000	0.02	+19000	+21000	+40000
10	1.75	0	0	0	0.07	1600	0	0	0	0
D 11	0.2	+120	+12000	+12000	0.08	1400	0.17	+122000	+134000	+253000
12	1.0	100	50000	30000	0.08	1400	0.14	96000	126000	238000
13	0.75	100	38000	22000	0.10	1200	0.17	96000	118000	223000
14	0.75	60	22000	13000	0.08	1500	0.08	59000	72000	136000
D 15	0.2	+40	+4000	+4000	0.37	3100	0.26	+40000	+44000	+83000
16	0.75	0	0	0	0.03	3300	0	0	0	0
17	0.75	0	0	0	0.03	3100	0	0	0	0
18	1.0	80	40000	24000	0.04	2900	0.06	79000	103000	195000
19	1.0	100	50000	30000	0.04	2700	0.07	98000	128000	242000
D 20	0.2	+20	+2000	+2000	0.04	260	0.01	+14000	+16000	+30000
21	1.0	20	10000	6000	0.04	2800	0.01	20000	26000	49000
22	1.0	30	15000	9000	0.04	3000	0.02	30000	39000	74000
23	1.5	70	52000	34000	0.04	3200	0.04	69000	103000	195000
24	1.0	80	40000	24000	0.03	3300	0.05	79000	103000	195000
25	2.0	30	30000	20000	0.03	3500	0.02	30000	50000	94000
26	1.0	80	40000	24000	0.03	3700	0.04	79000	103000	195000
D 27	0.4	+20	+4000	+4000	0.03	3700	0.01	+19000	+23000	+43000
28	0.75	0	0	0	0.03	3500	0	0	0	0
D 29	0.4	+20	+4000	+4000	0.03	3400	0.01	+19000	+23000	+43000
D 30	0.4	+20	+4000	+4000	0.03	3300	0.01	+19000	+23000	+43000
31	1.5	60	45000	29000	0.04	3200	0.04	59000	88000	166000
32	1.5	80	60000	39000	0.04	2800	0.06	79000	118000	223000
33	1.0	70	35000	21000	0.06	2000	0.07	69000	90000	170000
34	1.75	40	35000	21000	0.08	1400	0.06	39000	60000	113000
35	1.75	20	12000	8000	0.11	1000	0.04	20000	28000	53000
D 36	0.4	+40	+8000	+8000	0.09	1300	0.06	+38000	+46000	+87000
37	1.75	30	26000	18000	0.06	1800	0.03	30000	48000	91000
38	1.0	0	0	0	0.05	2300	0	0	0	0
39	1.0	20	10000	6000	0.04	2700	0.01	20000	26000	49000
40	1.5	20	15000	9000	0.04	3000	0.01	20000	29000	55000
41	1.0	20	10000	6000	0.03	3500	0.01	20000	26000	49000
42	1.5	30	22000	14000	0.03	3300	0.02	30000	44000	83000
43	1.0	90	45000	27000	0.03	3400	0.05	89000	116000	219000
44	1.75	100	75000	51000	0.04	3000	0.07	98000	149000	282000
45	1.75	120	90000	61000	0.03	3500	0.07	118000	179000	338000
46	1.5	110	82000	53000	0.03	3500	0.06	108000	161000	304000
D 47	0.4	+20	+4000	+4000	0.03	3300	0.01	+19000	+23000	+43000
48	1.5	0	0	0	0.03	3300	0	0	0	0
49	2.0	100	110000	77000	0.05	2200	0.10	107000	184000	348000
50	1.0	90	45000	27000	0.10	1100	0.16	86000	113000	214000
D 51	0.4	+30	+6000	+6000	0.06	1900	0.03	+29000	+35000	+66000
52	1.25	40	25000	16000	0.05	2200	0.04	40000	56000	106000
53	1.75	90	79000	53000	0.05	2300	0.08	88000	141000	266000
54	1.25	90	56000	35000	0.05	2300	0.08	88000	123000	232000
55	1.25	90	56000	35000	0.05	2300	0.08	88000	123000	232000

(sector13 continued)

56	1.25	100	62000	39000	0.06	2000	0.10	98000	137000	259000
57	1.25	120	75000	47000	0.09	1300	0.18	114000	161000	304000
58	1.25	100	62000	39000	0.10	1100	0.18	95000	134000	253000
59	1.5	0	0	0	0.06	1800	0	0	0	0
60	1.5	20	15000	10000	0.05	2200	0.02	20000	30000	57000
61	1.0	30	15000	9000	0.05	2100	0.03	30000	39000	74000
62	1.5	40	30000	20000	0.06	1900	0.04	39000	59000	111000
63	1.5	20	15000	9000	0.08	1500	0.03	20000	29000	55000
64	1.75	70	61000	41000	0.19	600	0.23	66000	107000	202000
TOTALS (x10 ³) :			1710	1072				2219	3291	6220

SECTOR # 14 Length: 28 km Average Retreat Rate : 1.7 m/yr

Segment No.	Onshore				Offshore				Totals	
	H	C	vi	v1	θ°	w	t	v2	volume	tons
1	1.75	20	17000	11000	0.08	1400	0.03	20000	31000	59000
2	1.75	0	0	0	0.08	1500	0	0	0	0
3	1.5	0	0	0	0.06	1800	0	0	0	0
4	1.25	20	12000	8000	0.06	1900	0.02	20000	28000	53000
5	1.75	30	26000	18000	0.07	1700	0.04	30000	48000	91000
6	2.25	0	0	0	0.07	1600	0	0	0	0
7	2.25	20	22000	16000	0.06	1800	0.02	20000	36000	68000
8	1.75	30	26000	18000	0.06	1800	0.03	30000	48000	91000
9	1.75	0	0	0	0.07	1700	0	0	0	0
10	1.75	20	17000	11000	0.06	1800	0.02	20000	31000	59000
11	1.5	0	0	0	0.06	1900	0	0	0	0
12	1.25	0	0	0	0.05	2200	0	0	0	0
13	1.25	20	12000	8000	0.04	2700	0.01	20000	28000	53000
D 14	0.4	+30	+6000	+6000	0.03	3300	0.02	+38000	+44000	+83000
D 15	0.4	+40	+8000	+8000	0.03	3500	0.02	+38000	+46000	+87000
16	2.25	20	22000	16000	0.03	4000	0.01	20000	36000	68000
17	2.25	20	22000	16000	0.02	4100	0.01	20000	36000	68000
18	1.25	60	37000	23000	0.03	3700	0.03	59000	82000	155000
19	1.25	40	25000	16000	0.03	4300	0.02	40000	56000	106000
20	2.25	0	0	0	0.02	5000	0	0	0	0
21	1.25	0	0	0	0.02	5400	0	0	0	0
22	0.75	0	0	0	0.02	5000	0	0	0	0
23	0.75	20	7000	4000	0.02	4600	0.01	20000	24000	45000
24	0.75	20	7000	4000	0.03	4500	0.01	20000	24000	45000
25	0.75	100	38000	22000	0.03	4200	0.05	99000	121000	229000
26	0.75	200	75000	44000	0.03	3700	0.11	194000	238000	450000
27	0.75	220	83000	49000	0.03	3400	0.13	213000	262000	495000
28	0.75	70	26000	15000	0.03	4000	0.04	69000	84000	159000
29	0.75	40	15000	9000	0.03	3500	0.02	40000	49000	93000
30	0.75	0	0	0	0.04	3000	0	0	0	0
31	0.75	70	26000	15000	0.04	3000	0.05	69000	84000	159000
32	0.75	100	38000	22000	0.04	3200	0.06	98000	120000	227000
A 33	0.75	50	19000	11000	0.03	3000	0.03	39000	50000	94000
A 34	0.75	200	75000	44000	0.02	3100	0.07	147000	191000	361000
A 35	0.75	210	79000	46000	0.03	2700	0.11	152000	198000	374000
A 36	0.75	180	68000	40000	0.03	2300	0.10	11000	51000	96000
A 37	0.75	0	0	0	0.03	2600	0	0	0	0
A 38	1.25	30	26000	16000	0.03	2600	0.01	11000	27000	51000
A 39	1.75	0	0	0	0.03	2500	0	0	0	0
A 40	1.75	20	17000	11000	0.03	2000	0.01	11000	22000	41000
A 41	1.75	0	0	0	0.04	1700	0	0	0	0
A 42	1.25	0	0	0	0.04	1500	0	0	0	0
A 43	0.75	0	0	0	0.05	1400	0	0	0	0
A 44	1.5	40	30000	20000	0.05	1300	0.03	20000	40000	76000
A 45	1.25	0	0	0	0.04	1700	0	0	0	0
A 46	1.75	0	0	0	0.03	2000	0	0	0	0
A 47	1.75	20	17000	11000	0.03	1700	0.01	9000	20000	38000
A 48	0.75	20	7000	4000	0.04	1400	0.01	7000	11000	21000
A 49	1.0	20	10000	6000	0.04	1300	0.01	7000	13000	24000
A 50	1.25	0	0	0	0.04	1500	0	0	0	0
A 51	1.25	0	0	0	0.03	1900	0	0	0	0
A 52	1.25	0	0	0	0.03	2000	0	0	0	0
A 53	1.25	0	0	0	0.03	1900	0	0	0	0
A 54	1.0	20	10000	6000	0.05	1200	0.02	11000	17000	32000
A 55	1.25	0	0	0	0.07	800	0	0	0	0
A 56	1.25	0	0	0	0.14	400	0	0	0	0
TOTALS ($\times 10^3$) :			897	546				1470	2016	3811

SECTOR # 15 Length: 36.5 km Average Retreat Rate : 1.0 m/yr

Pingok Island : segments measured clockwise around island from west end.


Segment No.	Onshore				Offshore				Totals	
	H	C	vi	v1	w	t	v2	volume	tons	
1	2.25	0	0	0	0.57	200	0	0	0	0
D 2	0.4	+20	+10000	+10000	0.67	170	0.59	+43000	+53000	+100000
D 3	0.4	+30	+6000	+6000	3.81	30	2.00	+15000	+21000	+40000
4	1.25	0	0	0	1.64	70	0	0	0	0
D 5	0.4	+130	+26000	+26000	2.29	50	5.19	+130000	+156000	+295000
D 6	0.4	+120	+24000	+24000	2.29	50	4.79	+120000	+144000	+272000
7	0.75	0	0	0	1.43	80	0	0	0	0
D 8	0.4	+20	+4000	+4000	1.43	80	0.50	+20000	+24000	+45000
D 9	0.4	+30	+6000	+6000	1.43	80	0.75	+30000	+36000	+68000
D 10	0.4	+40	+8000	+8000	1.04	110	0.73	+40000	+48000	+91000
11	1.75	40	35000	24000	1.43	80	1.00	30000	54000	102000
12	1.75	20	18000	12000	1.15	100	0.40	18000	30000	57000
13	1.75	80	70000	47000	0.95	120	1.33	53000	100000	189000
B 14	0.5	100	25000	14000	2.29	50	2.00	100000	114000	215000
15	0.5	100	25000	14000	0.10	1200	0.17	96000	110000	208000
16	1.75	100	88000	59000	0.10	1200	0.17	96000	155000	293000
17	1.75	100	88000	59000	0.13	900	0.22	94000	153000	289000
18	1.75	110	96000	65000	0.23	500	0.44	98000	163000	308000
19	1.75	100	88000	59000	0.16	700	0.29	93000	152000	287000
20	1.75	100	88000	59000	0.15	750	0.27	93000	152000	287000
21	1.75	100	88000	59000	0.14	800	0.25	94000	153000	289000
22	1.75	100	70000	47000	0.11	1000	0.20	95000	142000	268000
23	2.0	80	70000	49000	0.08	1400	0.11	78000	127000	240000
24	1.75	90	79000	53000	0.07	1750	0.10	88000	141000	266000
25	1.75	60	52000	35000	0.06	1950	0.06	59000	94000	178000
26	1.25	80	50000	31000	0.06	1950	0.08	78000	109000	206000
27	1.25	80	50000	31000	0.06	1900	0.08	78000	109000	206000
28	1.25	100	63000	39000	0.07	1650	0.12	97000	136000	257000
29	2.25	80	90000	64000	0.06	1850	0.09	78000	142000	268000
30	2.25	100	112000	80000	0.06	1800	0.11	97000	177000	335000
31	2.25	30	34000	24000	0.05	2500	0.02	30000	54000	102000

Offshore input from removal of bar : 17000 17000 32000

////////////////////////////////////

(sector 15 continued)


Bertoncini and Bodfish Islands : segments measured clockwise from west end.

Segment No.	Onshore				Offshore				Totals	
	H	C	vi	v1	 w	t	v2	volume	tons	
B 1	1.75	120	105000	71000	0.95	40	2.00	120000	191000	361000
B 2	1.75	100	88000	59000	1.14	50	2.00	100000	159000	301000
B 3	2.25	120	135000	97000	0.95	40	2.00	120000	217000	410000
B 4	2.25	100	112000	80000	1.14	90	2.00	100000	180000	340000
5	1.75	70	61000	41000	0.57	200	0.70	58000	99000	187000
D 6	0.4	+50	+10000	+10000	0.14	775	0.12	+49000	+59000	+112000
7	1.75	40	0	0	2.86	0	0	0	0	0
D 8	0.4	+20	+4000	+4000	0.14	800	0.05	+20000	+24000	+45000
D 9	0.4	+20	+4000	+4000	0.13	900	0.04	+18000	+22000	+42000
D 10	0.4	+60	+12000	+12000	0.09	1300	0.01	+6000	+18000	+34000
D 11	0.4	+20	+4000	+4000	0.06	1800	0.02	+19000	+23000	+43000
D 12	0.4	+110	+22000	+22000	0.07	1700	0.13	+106000	+128000	+242000
13	2.25	0	0	0	0.09	1200	0	0	0	0

////////////////////////////////////

(sector 15 continued)

Cottle Island : segments measured clockwise from west end.

Segment No.	Onshore				Offshore				Totals	
	H	C	vi	v1		w	t	v2	volume	tons
1	1.75	0	0	0	0.76	150	0	0	0	0
2	1.75	20	17000	11000	1.15	100	0.40	18000	29000	55000
3	1.75	40	35000	24000	1.15	100	0.80	32000	56000	106000
4	1.75	0	0	0	0.72	160	0	0	0	0
5	1.75	50	44000	30000	1.15	100	1.00	37000	67000	127000
6	1.75	50	44000	30000	2.3	50	2.00	25000	55000	104000
7	1.75	60	52000	35000	1.64	70	1.71	34000	69000	130000
8	1.75	90	79000	53000	1.27	90	2.00	45000	98000	185000
9	1.75	60	52000	35000	1.64	70	1.70	34000	69000	130000
10	1.75	40	35000	24000	0.76	150	0.53	35000	59000	112000
11	1.75	0	0	0	0.52	220	0	0	0	0
12	1.75	20	17000	11000	0.57	200	0.20	19000	30000	57000
13	1.75	0	0	0	0.38	300	0	0	0	0
14	1.75	0	0	0	0.10	1100	0	0	0	0
15	1.75	100	88000	59000	0.08	1400	0.14	96000	155000	293000
16	1.75	50	44000	30000	0.08	1500	0.07	49000	79000	149000
17	1.75	0	0	0	0	0	0	0	0	0
D 18	0.4	+70	+7000	+7000	0.10	1100	0.12	+69000	+76000	+144000
19	1.75	0	0	0	0.13	900	0	0	0	0
20	1.75	80	88000	59000	0.10	1200	0.13	77000	136000	257000
21	1.75	50	44000	30000	0.08	1500	0.07	49000	79000	149000
22	1.75	0	0	0	0.08	1400	0	0	0	0
23	1.75	0	0	0	0.08	1300	0	0	0	0
D 24	0.4	+20	+4000	+4000	0.08	1400	0.03	+21000	+25000	+47000
25	1.75	20	17000	11000	0.07	1600	0.03	20000	31000	59000
26	1.75	30	26000	18000	0.08	1500	0.04	30000	48000	91000
27	1.75	0	0	0	0.07	1600	0	0	0	0
28	1.75	0	0	0	0.07	1600	0	0	0	0
29	1.75	0	0	0	0.07	1600	0	0	0	0

Input not calculated for Thetis, Spy, Leavitt, Stump, Egg, and Long islands; no net change.

TOTALS ($\times 10^3$) : 2428 1581 2052 3633 6866

REFERENCES CITED

- Arden, R.S. and Wigle, T.S., 1972, Dynamics of ice formation in the upper Niagra River, in International Symposium on the Role of Snow and Ice in Hydrology, Banff, Alberta: v. 2, UNESCO-WMO-IHAS, p. 1296-1313.
- Arnborg, L., Walker, H.J., and Peippo, J., 1967, Suspended load in the Colville River, Alaska, 1962: *Geografiska Annaler*, v. 49, no. A, p. 131-144.
- Barnes, P. W. and Reimnitz, Erk, 1973, The shore fast ice cover and its influence on the currents and sediment along the coast of northern Alaska: EOS, American Geophysical Union, v. 54, p. 1108.
- Barnes, P. W. and Reimnitz, Erk, 1974, Sedimentary processes on arctic shelves off the northern coast of Alaska, in *The Coast and Shelf of the Beaufort Sea: The Arctic Institute of North America*, Arlington, Va., p. 439-476.
- Barnes, P.W., Reimnitz, Erk, Smith, G., and Melchior, J., 1977, Bathymetric and shoreline changes, northwestern Prudhoe Bay, Alaska: U.S. Geological Survey Open-File Report 77-16715.
- Barnes, P.W., McDowell, D., and Reimnitz, Erk, 1978, Ice gouging characteristics: Their changing patterns from 1975-1977, Beaufort Sea, Alaska: U.S. Geological Survey Open-File Report 78-73042.
- Barnes, P. W. and Reimnitz, Erk, 1979, Ice gouge obliteration and sediment redistribution event; 1977-1978, Beaufort Sea, Alaska: Open File Report 79-848, U.S.G.S. Department of the Interior.
- Barnes, P. W., 1982, Marine ice-pushed boulder ridge: *Arctic*, v. 35, no. 2, p. 312-316.
- Barnes, P.W., Rearic, Douglas M., and Reimnitz, Erk, 1984, Ice gouging characteristics and processes, in *The Alaskan Beaufort Sea: ecosystems and environments: Academic Press Inc.*, p. 185- 212.
- Black, R.E. and Barksdale, W.E., 1949, Oriented lakes of northern Alaska: *Journal of Geology*, v. 57, p. 105-118.
- Black, R.F., 1964, Gubik Formation of Quaternary age in northern Alaska: Professional Paper 302-C91, U.S. Geological Survey .
- Brigham, J. K., Hopkins, D. M., Carter, L. D., and Miller, G. H., 1980, Application of amino acid geochronology to deposits of the arctic coastal plain, Alaska: preliminary results and implications: Preceedings of the ninth annual arctic workshop april 4 and 5 198034-35, INSTAAR, University of Colorado.
- Bruun, Per, 1962, Sea level rise as cause of shore erosion: American Society of Civil Engineers Proceedings, *Journal of the Waterways and Harbors Division*, v. 88, no. WW1, p. 117-130.
- Cannon, P.J. and Rawlinson, S.E., 1978, The environmental geology and geomorphology of the barrier island-lagoon system along the Beaufort Sea coastal plain from Prudhoe Bay to the Colville River: Boulder, Co, National Oceanic and Atmospheric Administration, .

- Cannon, P.J., 1979, The environmental geology and geomorphology of the barrier island-lagoon system along the Beaufort Sea coastal plain: Environmental Assessment of the Alaskan Continental Shelf, Annual Reports 209-248, National Oceanic and Atmospheric Administration.
- Cannon, P.J., 1979, The environmental geology and geomorphology of the barrier island-lagoon system along the Beaufort Sea coastal plain, in Environmental Assessment of the Alaskan Continental Shelf, Annual Reports: v. 10, p. 209-248.
- Carson, C.E. and Hussey, K.M., 1959, The multiple-working hypothesis as applied to Alaska's oriented lakes: Proceedings of the Iowa Academy of Sciences, v. 66, p. 334-349.
- Carson, C.E. and Hussey, K.M., 1962, The oriented lakes of arctic Alaska: Journal of Geology, v. 70, p. 417-439.
- Carter, L. David and Robinson, Stephen W., 1980, Minimum age of beach deposits north of Teshekpuk Lake, Alaskan arctic coastal plain: U.S. Geological Survey in Alaska, Accomplishments during 1979, Geological Survey Circular 823-B, p. B8-B9.
- Carter, David L., 1983, Cenozoic glacial and glaciomarine deposits of the central north slope, Alaska, in Glaciation in Alaska: extended abstracts from a workshop: Alaskan Quaternary Center, University of Alaska Museum, .
- Curry, J.R., 1964, Transgressions and regressions, in Papers in marine geology- Shepard Commemorative Volume: McMillan Co., New York, p. 175-203.
- Dionne, J.C., 1973, La notion de pied de glace (icefoot), en particulier dans l'estuaire du Saint-Laurent: Cahiers de Geographie de Quebec, v. 17, no. 41, p. 221-250.
- Dunton, Kenneth H., Reimnitz, Erk, and Schonberg, Susan, 1982, An arctic kelp community in the Alaskan Beaufort Sea: Arctic, v. 35, no. 4, p. 465-484.
- Dygas, J.A., Tucker, R., and Burrell, D.C., 1972, Geologic report of the heavy minerals, sediment transport, and shoreline changes of the barrier islands and coast between Oliktok Point and Beechey Point, in Baseline Data Study of the Alaskan Arctic Aquatic Environment; University of Alaska International Marine Sciences Report R-72 3: p. 62-121.
- Dygas, J.A. and Burrell, D.C., 1976, Dynamic sedimentological processes along the Beaufort Sea coast of Alaska, in Assessment of the Arctic Marine Environment: Selected Topics: Institute of Marine Sciences, University of Alaska, Fairbanks, Alaska., p. 189-203.
- Forbes, D.L., 1981, Babbage River delta and lagoon: hydrology and sedimentology of an arctic estuarine system, in Unpub. Ph.D. Dissertation: Dept. of Geography, Univ. of British Columbia, Vancouver B.C., p. 554.
- Harper, J.R., Owens, E.H., and Jr., W.J. Wiseman, 1978, Arctic beach processes and the thaw of ice-bonded sediments in the littoral zone, in Proceedings of the 3rd International Permafrost Conference: National Academy of Sciences, Washington, D.C., p. 195-199.
- Harper, J.R., 1978, The physical processes affecting the stability of tundra cliff coasts, in Unpublished Ph.D. thesis: Louisiana State University, Baton Rouge, LA., p. 212.
- Harrison, W. D. and Osterkamp, T. E., 1981, Subsea permafrost: probing, thermal regime and data analysis: Environmental Assessment of the Alaskan Continental Shelf, Annual Reports

- of Principal Investigators for the year, U.S. Department of Interior, v. VII: Hazards, p. 291-350.
- Hartz, R.W., 1978, Erosional hazards map of the arctic coast of the National Petroleum Reserve, Alaska: U.S. Geological Survey Open-File Report 78-4068.
- Hodel, Karen, 1985, Microfeatures of quartz grains from modern Arctic terrestrial and subaqueous environments, North Slope, Alaska: (unpublished Master's Thesis), University of California, Berkeley, p. 69.
- Holmquist, Charlotte, 1978, Lakes of polar regions: age, complexity, and trophic state: Proceedings of the International Association of Theoretical and Applied Limnologists, v. 20, no. 1, p. 615-617.
- Hopkins, D.M. and Hartz, R.W., 1978, Coastal morphology, coastal erosion and barrier islands of the Beaufort Sea, Alaska: U.S. Geological Survey Open-File Report 78-106354.
- Carter, D.M. Hopkins and L.D., 1980, Discrepancy in correlation of transgressive marine deposits of Alaska and the eastern arctic, in Proceedings of the 9th Annual Arctic Workshop: INSTAAR, University of Colorado, Boulder, Colorado, p. 12-13.
- Inman, D. L. and Chamberlain, T. K., 1960, Littoral sand budget along the southern California coast, in Report of the Twenty-first Int. Geol. Cong. abstracts: Copenhagen, .
- Inman, D. L. and Brush, B. M., The coastal challenge: Science, v. 181, p. 20-32.
- Klyuyev, Ye. V., 1965, The role of permafrost factors in the dynamics of bottom topography in polar seas: Oceanology of the Academy of Sciences of the U.S.S.R., v. 5, no. 1, p. 78-83.
- Kobayashi, Nobuhisa, Vivatrat, Vitoon, Watt, Brian, Madsen, Ole S., and Boaz, Irvin B., 1981, Erosion prediction for exploration and production structures in the arctic: Offshore Technology Conference, 13th annual meeting, Houston, Texas, v. OTC paper 4114.
- Kovacs, Austin, 1983, Shore ice ride-up and pile-up features, Part I: Alaska's Beaufort Sea coast: CRREL Report 83-959, U.S. Army Corp of Engineers, Hanover, New Hampshire.
- Kovacs, Austin, 1984, Shore ice ride-up and pile-up features, Part II: Alaska Beaufort Sea coast - 1983 and 1984: CRREL Report 84-2629, U.S. Army Corps of Engineers, Hanover, New Hampshire.
- Lachenbruch, Arthur T., 1985, Temperature and Depth of Permafrost on North Slope, Alaska: American Association of Petroleum Geologists, Bulletin, v. 69, no. 4, p. 667-668.
- Lachenbruch, Arthur T., Sass, J.H., Marshall, B.V., and Jr., T.H. Moses, 1982, Permafrost, heat flow, and the geothermal regime at Prudhoe Bay, Alaska: Journal of Geophysical Research, v. 87, no. B11, p. 9301-9316.
- Lee, Homa J. and Winters, William J., 1984, Strength and consolidation properties of stiff Beaufort Sea sediment: Proceedings, Arctic Energy Technologies Workshop, November 14-15 1984, U.S. Department of Energy, Office of Fossil Energy Morgantown Energy Technology Center.

- Leffingwell, E. deK., 1919, The Canning River region, northern Alaska: U.S. Geological Survey Professional Paper 109251.
- Lewellen, R.I., 1977, A study of Beaufort Sea coastal erosion, northern Alaska: P.O. Box 2435, Littleton Co., Published by the Author, .
- Livingstone, D.A., 1954, On the orientation of lake basins: American Journal of Science, v. 252, p. 547-554.
- Martin, Seelye, 1981, Frazil ice in rivers and oceans, in Ann. Rev. Fluid Mech.: v. 13, p. 379-397 :I Annual Reviews Inc..
- Martin, Seelye, 1981, Frazil ice in rivers and oceans: Revue of Fluid Mechanics, v. 13, p. 379-397.
- Matthews, J.B., 1981, Circulation in the Sale 71 area: Beaufort Sea Sale 71 Synthesis Report 71-178, National Oceanic & Atmospheric Administration, Boulder, CO.
- May, S. Kimball, Dolan, Robert, and Hayden, Bruce P., 1983, Erosion of U.S. shorelines: EOS, Transactions, American Geophysical Union, p. 521-522.
- McDonald, B.C. and Lewis, C.P., 1973, Geomorphic and sedimentologic processes of rivers and coasts, Yukon coastal plain: Env.-Social Comm., Northern Pipeline, Task Force on Northern Oil Dev., Report 73-79245.
- Morack, J.L. and Rogers, J.C., 1981, Seismic evidence of shallow permafrost beneath islands in the Beaufort Sea, Alaska: Arctic, v. 34, no. 2, p. 169, 174.
- Moore, J. Robert, Buck, Beaumont, Gerwick, Ben C. Jr., Judge, Alan S., Lewis, C. F. Michael, Runge, Karl H., Sellmann, Paul V., and Watt, Brian J., 1982, Understanding the arctic sea floor for engineering purposes: Committe on Arctic Seafloor Engineering, Marine Board Commission on Engineering and Technical Systems, National Research Council , National Academy Press.
- Naidu, A. S. and Mowatt, T. C., 1983, Sources and dispersal patterns of clay minerals in surface sediments from the continental- shelf areas off Alaska: Geological Society of America Bulletin, v. 94, p. 841-854.
- Naidu, A. S., Mowatt, T. C., Rawlinson, Stuart E., and Weiss, Herbert V., 1984, Sediment characteristics of the lagoons of the Alaskan Beaufort Sea coast and evolution of Simpson Lagoon, in The Alaskan Beaufort Sea: Ecosystems and Environments: Academic Press Inc., p. 275.
- Nummedal, D., 1979, Coarse-grained sediment dynamics - Beaufort Sea, Alaska., in Proceedings of port and ocean engineering under arctic conditions: Norwegian Institute of Technology, p. 845-858.
- Osterkamp, T.E., 1978, Frazil ice formation: a review: Journal of the Hydraulics Division, ASCE, v. 104, no. HY9, p. 1239-1255.
- Osterkamp, T.E. and Gosink, Joan P., 1984, Observations and analyses of sediment laden sea ice, in The Alaskan Beaufort Sea: ecosystems and environments: Acadaemic Press Inc., p. 73-94.
- Owens, E.H. and Harper, J.R., 1977, Frost-table and thaw depth in the littoral zone near Peard

- Bay, Alaska.: *Arctic*, v. 30, no. 3, p. 155-168.
- Owens, E. H., Harper, J. R., and Nummedal, D., 1980, Sediment transport processes and coastal variability on the Alaskan North Slope, in *Proceedings of the 17th International Coastal Engineering Conference* : ASCE, Sydney, Australia, p. 1344-1363.
- Owens, E.H., 1982, Ice foot, in *Encyclopedia of Beaches and Coastal Environments*: Hutchinson Ross Publ. Co., Stroudsburg, Pa., p. 480-481.
- Reimnitz, Erk and Bruder, K.F., 1972, River discharge into an ice-covered ocean and related sediment dispersal, Beaufort Sea, coast of Alaska: *Geological Society of America Bulletin*, v. 83, no. 3, p. 861-866.
- Reimnitz, Erk and Barnes, P.W., 1974, Sea ice as a geologic agent on the Beaufort Sea shelf of Alaska, in *The Coast and Shelf of the Beaufort Sea. Proceedings of the Arctic Institute of North America Symposium on Beaufort Sea and Shelf Research*: Arctic Institute of North America, Arlington, Va., p. 301-353.
- Reimnitz, Erk and Maurer, D.K., 1979, Effects of storm surges on the Beaufort Sea coast, northern Alaska: *Arctic*, v. 32, no. 4, p. 329-344.
- Reimnitz, Erk and Kempema, E.W., 1982, Dynamic ice-wallow relief in northern Alaska's nearshore: *Journal of Sedimentary Petrology*, v. 52, no. 2, p. 451-462.
- Reimnitz, Erk and Kempema, E.W., 1983, High rates of bedload transport measured from the infilling rate of large strudel-scour craters in the Beaufort Sea, Alaska: *Continental Shelf Research*, v. 1, no. 3, p. 237-251, plus erratum in next issue for missing page.
- Reimnitz, Erk, Toimil, L.J., and Barnes, P.W., Arctic continental shelf morphology related to sea-ice zonation, Beaufort Sea, Alaska: *Marine Geology*, v. 28, p. 179-210.
- Rex, R.W., 1961, Hydrodynamic analysis of circulation and orientation of lakes in northern Alaska: *Geol. Arct.*, v. 2, p. 1021-1043.
- Rosen, Peter S., 1978, A regional test of the "Bruun Rule" on shoreline erosion: *Marine Geology*, v. 26, p. M7-M16.
- Rosen, Peter S., 1978, Predicting beach erosion as a function of rising water level: Discussion: *Journal Of Geology*, v. 86, no. 6, p. 763-764.
- Schwartz, Maurice L., 1967, The "Bruun Theory" of sea-level rise as a cause of shore erosion: *Journal Of Geology*, v. 75, no. 1, p. 76-92.
- Sejrup, Hans Peter, Miller, Gifford H., Brigham-Grette, Julie, Lovlie, Reidar, and Hopkins, David, 1984, Amino acid epimerization implies rapid sedimentation rates in Arctic Ocean cores: *Nature*, v. 310, p. 772-775.
- Sellmann, P. V., Brown, J., Lewellen, R., McKim, H., and Merry, C., 1975, The classification and geomorphic implications of thaw lakes on the arctic coastal plain, Alaska.: CRREL Research Report 34421, U.S. Army Corp of Engineers, Hanover, New Hampshire.
- Sellmann, P.V., Weeks, W.F., and Campbell, W.J., 1975, Use of side-looking airborne radar to

determine lake depth on the Alaskan North Slope, in Cold Regions Research and Engineering Laboratory, Special Report 230: p. 6.

- Short, A. D., Coleman, J. M., and Wright, L. D., 1974, Beach dynamics and nearshore morphology of the Beaufort Sea coast, Alaska, in *The Coast and Shelf of the Beaufort Sea: The Arctic Institute of North America*, Arlington, Va., p. 477-488.
- Swift, Donald J. P., 1968, Coastal erosion and transgressive stratigraphy: *Journal of Geology*, v. 76, p. 444-456.
- Taylor, R.B., 1980, Beach thaw depth and the effect of ice-bonded sediment on beach stability, in *Proceedings of the Canadian Coastal Conference*, Burlington, Ontario, April 22-24, 1980: p. 103-121.
- Tedrow, J.C.F., 1969, Thaw lakes, thaw sinks and soils in northern Alaska: *Biuletyn Per-glacjalny*, v. 20, p. 337-344.
- Tomirdiaro, S.V., 1975 *J% DOKLADY*, Earth Science Sections, , Thermoabrasion-induced shelf formation in the eastern arctic seas of the USSR during the Holocene: , v. 219, no. 1-6, 23-26.
- Tsang, Gee, 1982, Frazil and anchor ice: a monograph: Ottawa, Ontario Canada, NRC Subcommittee on hydraulics of ice covered rivers, 90 .
- Weeks, W.F. and Weller, G., July 1984, Offshore oil in the Alaskan Arctic: *Science*, v. 225, no. 4660, p. 371-378.
- Weller, M.W. and Derksen, D.V., 1979, The geomorphology of Teshekpuk Lake in relation to coastline configuration of Alaska's coastal plain: *Arctic*, v. 32, no. 2, p. 152-160.
- Williams, J.R., Yeend, W.E., Carter, L.D., and Hamilton, T.D., 1977, Alaska: U.S. Geological Survey Open-File Report 77-868.
- Winant, Clinton D., Inman, Douglas L., and Nordstrom, Charles E., 1975, Description of seasonal beach changes using empirical eigenfunctions: *Journal of Geophysical Research*, v. 80, no. 15, p. 1979.
- Wiseman, W.J., Coleman, J.M., Gregory, A., Hsu, S.A., Short, A.D., Suhayda, J.N., Walters, C.D., and Wright, L.D., 1973, Alaskan arctic coastal processes and morphology: Tech. Rept. 149171, Louisiana State University, Baton Rouge, LA..